

## Laboratory studies of double-diffusive sources in closed regions

By J. S. TURNER<sup>1</sup> AND G. VERONIS<sup>2</sup>

<sup>1</sup>Research School of Earth Sciences, Australian National University, Canberra,  
ACT 0200, Australia

<sup>2</sup>Kline Geological Laboratory, Yale University, New Haven, CT 06520-8109, USA

(Received 11 May 1999 and in revised form 15 October 1999)

Various observations of layering and intrusions in the ocean strongly suggest that such structures and motions are produced and driven by horizontal and vertical gradients of temperature and salinity, i.e. by double-diffusive processes. Much of the laboratory work in this field has concentrated on one-dimensional problems, with the neglect of two-dimensional phenomena. The latter are addressed explicitly in the present paper, using the salt–sugar analogue system in a simple geometry, but with the aim of establishing some more widely applicable general principles. Two sources of salt or sugar solution were fed in at opposite ends of a 750 mm long tank, with an overflow tube drawing fluid from a point at the centre of the tank. With two salt sources of different concentrations and densities, a stratification built up through the ‘filling box’ process, and the total density range lay within that of the input solutions. For one salt and one sugar source, a much larger density gradient could be set up, with the range lying outside that of the inputs. The flows were monitored using various experimental techniques: photographs of dye streaks with still and video cameras; a polarimeter to monitor sugar concentration; and the withdrawal of samples for the measurement of density and refractive index, from which the separate contributions of salt and sugar to the density could be calculated.

Three related experiments with simple input conditions were particularly instructive, and these will be described first. Both inputs and the withdrawal tube were located at mid-depth, and the tank fluid and the salt and sugar supplies had the same density. The only difference between runs was the initial composition of the solution in the tank: pure salt, pure sugar, and a 50 : 50 mixture of the two. Following an initial transient response which was different in the three experiments, they all tended to the same asymptotic distributions of salt, sugar and density after about 100 h, with a sharp central interface and weakly stratified upper and lower layers. This state corresponded approximately to the one-dimensional ‘rundown’ of a layer of salt solution above sugar solution, with a slightly higher, unstable concentration of salt in the top layer compared to the bottom and a very stable sugar distribution, with a much larger concentration in the bottom layer than in the top one. This distribution cannot be produced by ‘finger’ rundown, and it corresponds to the maximum release of potential energy. It was, however, achieved through the action of many intrusions, which remained active in the dynamic final state, and maintained a strong communication between the two ends of the tank. A comparable experiment was carried out using a tank 1820 mm long. With this larger aspect ratio there was a predominantly local influence of the sources at each end of the tank. Other runs have explored a variety of geometries of the sources and sinks, and the final state has been shown to be sensitive to these boundary conditions.

---

## 1. Introduction

It is a truism to say that both the stratification of the ocean and the thermohaline circulations within it are ultimately determined by the geometry, strengths and nature of all the localized and distributed sources and sinks of heat and salt near the surface. The bottom water of all the world's oceans is known to form in just a few limited regions: Antarctic Bottom Water in the Weddell Sea, and North Atlantic Deep Water in the Greenland and Norwegian Seas. The basic features of the formation process can be understood in terms of a very simple theoretical and laboratory model. Baines & Turner (1969) showed that the continued supply of dense fluid from a small source at the surface of a closed region of initially homogeneous fluid produces a stable density gradient, and they calculated the form and magnitude of this in a region of constant cross-section and uniform depth. The 'filling box' effect due to a single plume of salt solution feeding into a tank of fresh water was also documented in their laboratory experiments. Wong & Griffiths (2000) have extended those experiments, and the corresponding theory, to determine the effect of multiple plumes feeding into a long tank at different horizontally-separated positions.

The water right at the bottom of the ocean must correspond to the localized source which, after entraining lighter water at shallower depths, arrives at the bottom with the highest density. For vertical plumes (as in many laboratory experiments), or on a fixed slope, this will be the source having the largest buoyancy flux, but steeper slopes will produce more mixing, so both the density and the volume flux need to be considered separately. The mean stratification adjusts to the bottom influx, with the effects of the resulting upwelling being balanced by distributed downward fluxes from the surface. Sources with smaller buoyancy fluxes (or more mixing) cannot penetrate to the bottom of the density gradient set up by the densest source of bottom water, and so they spread out at shallower depths. Thus inputs from marginal seas such as the Mediterranean, which has a smaller buoyancy flux and flows down a steep slope, entraining more lighter water from the density gradient set up by the major sources, become neutrally buoyant before they reach the bottom, and spread out as intrusions at mid-depth.

In addition to the 'filling box' models mentioned above, there has been some theoretical and laboratory work on flows driven by horizontal gradients of buoyancy, particularly in the context of estuaries or gulfs. Phillips (1966), for example, considered the buoyancy-driven circulation in the Red Sea produced by surface cooling, and Maxworthy (1997) has reviewed and extended subsequent models of convection into domains with open boundaries. Rossby (1965), with the problem of deep convection in the ocean in mind, studied the convection driven by a linear temperature gradient maintained along the bottom of a laboratory tank, and showed that this resulted in a single overturning cell. Pierce & Rhines (1996) have used a laboratory model to examine the development of stratification as well as the circulations in a long tank, with surface fluxes of fresh water supplied at one end and salt water at the other. This, and their related numerical model, were explicitly aimed at understanding the ocean's thermohaline circulation, forced by surface buoyancy fluxes.

There are relatively few such experiments using spatially separated sources, even in the simplest case with a single stratifying property, and neglecting diffusion. Oceanic sources, however, are inherently double-diffusive because of their different temperatures and salinities. Even the most basic schematic picture of the sources and north-south distribution of the major water masses (for example in the North Atlantic) distinguishes these through their different  $T/S$  properties and shows tongues

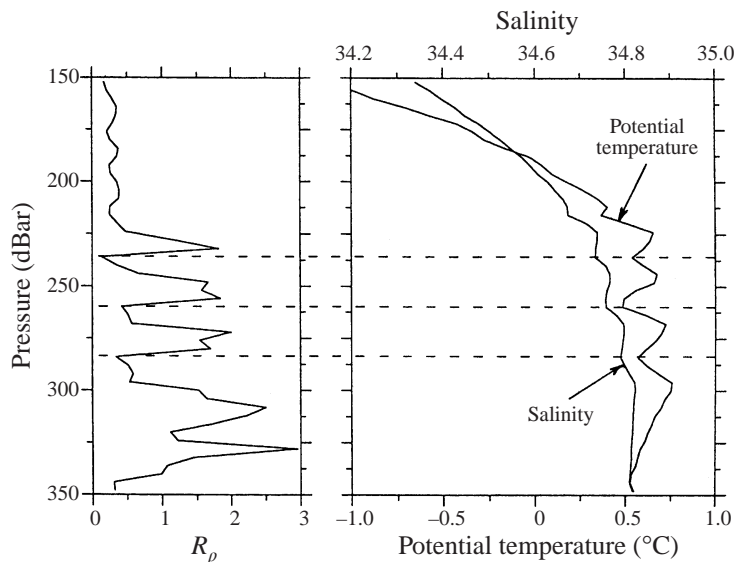


FIGURE 1. Vertical profiles of temperature, salinity and density ratio  $R_p$ , at a station at the edge of the Canada Basin. (From Carmack *et al.* (1997), which reports the results of the Canada/US 1994 Arctic Ocean Section experiment.)

of water with higher and lower temperatures and salinities interleaving at different depths. There are several recent striking observations of spatially extensive structures which have been interpreted and discussed in terms of double-diffusive processes. Two of these will now be summarized, to provide some specific oceanographic motivation for the present laboratory work.

Schmitt (1994) has reported and analysed the results of a large-scale survey of double-diffusive layers in the Caribbean in 1985 (C-SALT). There are salt fingers across the interfaces between well-mixed layers 5–40 m deep; they are horizontally extensive, and exist between a southward-flowing salinity maximum and a northward-flowing salinity minimum. The persistence of these layers and their properties have been attributed to the action of horizontal and vertical gradients of  $T$  and  $S$ , combined with vertical transport by fingers, and Schmitt has explicitly compared these observations with the laboratory experiments on counterflowing layers reported by Turner & Chen (1974), referred to below.

Carmack *et al.* (1997) have reported measurements in the Arctic Ocean which show that a major (and continuing) warming has taken place during the 1990s, due to influx of anomalously warm waters from the Atlantic. The transition is occurring via persistent multiple intrusions, 40–60 m thick, extending laterally in a coherent manner through the Atlantic water and upper deep waters of the Arctic. (See figure 1.) The authors note that these layers can support both diffusive and finger convection, and they believe that they are self-organizing and self-propelled by these double-diffusive transports.

## 2. Previous experiments using double-diffusive sources

The few laboratory experiments in which two-dimensional effects of double diffusion have been explored have mainly used the sugar/salt analogue for salinity and temperature differences. Turner & Chen (1974) examined the effects of hori-

zontal gradients of properties in various geometries, and their observations can be regarded as a qualitative prelude to the present experiments. Turner (1978) reported observations on intrusions produced by localized sources of salt or sugar feeding into a salinity gradient. The behaviour is very different without and with double diffusion – in the latter case strong vertical convection occurs, with the spread of intrusions moving across isopycnals at many levels.

Vertical boundaries or fronts with different diffusive properties across them have also been studied. Ruddick & Turner (1979) observed the formation of intrusions across a laboratory front with stable gradients of sugar on one side and salt on the other, but identical vertical density gradients. Further experiments in this geometry, together with a theoretical interpretation of the major features of the flow, have recently been reported by Ruddick, Phillips & Turner (2000). There have been several studies of the layers formed by heating the sidewall of a tank containing a solute gradient (see Chen & Chen 1997 for a recent example, and references to earlier work). Huppert & Turner (1980) reported an experimental study of iceblocks melting into a salinity gradient, which produced both temperature and salinity anomalies. Turner (1998) has recently carried out a laboratory study of an 'inverse estuary', in which heating and evaporation on a shelf produced vertical stratification and circulations in an initially homogeneous tank, with strong double-diffusive effects dominating.

The experiments to be described in the present paper can be regarded as the double-diffusive equivalent of those reported by Pierce & Rhines (1996). Instead of using small source regions of salty and fresh water, at opposite ends of a long tank containing saline solution of intermediate density, the source fluids used are now salt and sugar solutions. These produce dramatically different effects from those possible with a single solute, and the experiments provide a convenient way to explore some fundamental processes which can become important in any double-diffusive system. The aim is to establish general principles which can be applied whenever spatially non-uniform temperature and salinity anomalies (or the analogue salinity and sugar differences) are present in a confined region. We also hope to draw the attention of oceanographers to potentially important processes which they might look for and study in the ocean.

### **3. Experimental method**

Most of the new experiments were carried out in a Perspex tank 750 mm long, 75 mm wide and 250 mm deep, initially filled to a depth of about 150 mm with homogeneous salt or sugar solution. The input fluids were supplied near the two ends of the tank through 2 mm diameter plastic tubing connected to large reservoirs, with the outlets usually directed horizontally at various depths in different runs. The flow rates were small and the same for the two inputs, in the range 5–10 ml min<sup>-1</sup>, and were controlled using a peristaltic pump with two identical heads. The volume of fluid in the tank was kept constant using a simple constant-head overflow device, the inlet to which was at the centre of the tank, and placed at any desired depth. The volume of the overflow was measured at intervals to give a direct measure of the total input rate. A schematic view of the experimental setup is shown in figure 2.

The developing motions were followed by dropping in dye crystals to produce vertical streaks and monitoring their distortion. Photographs were taken either against a uniformly lit white background, or using a shadowgraph. In some long runs a time-lapse video recording was made for later analysis, and dye streaks were dropped in using a mechanical device which could be programmed to operate at any desired times.

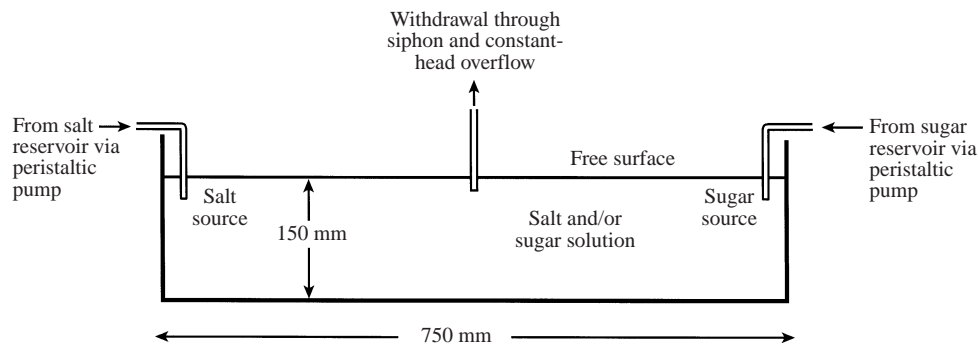


FIGURE 2. Sketch of the experimental tank.

The time history of the vertical stratification, and the separate contributions of sugar and salt to the density, were measured using small samples withdrawn from standard depths at several positions along the tank. For each sample, the refractive index was determined (to 1 part in  $10^4$ ) using a hand-held refractometer and the density (more accurately, to 1 part in  $10^5$ ) using an Anton Paar densitometer. Each pair of readings was then used to calculate the corresponding salt and sugar concentrations, using the procedure developed by Ruddick & Shirtcliffe (1979). It was the lack of such a method for obtaining accurate property values that prevented Turner & Chen (1974) from pursuing the quantitative aspects of the exploratory experiments they described.

A series of runs using different geometries for the sources and sinks, and various tank and source compositions, will now be discussed. These have been chosen, from a total of 24 runs carried out over a period of several years, to illustrate the major points. They will be presented in a sequence which emphasizes the most striking features of the experiments and the conclusions drawn from them. Table 1 gives a summary of the input conditions used in all the runs which are discussed in this paper. The unit of density is  $\text{g cm}^{-3}$ .

#### 4. 'Control' experiment

Run A was the closest in the present geometry to the conditions used by Pierce & Rhines (1996). That is, the sources were both salt solutions, one lighter ( $\rho = 1.098 \text{ g cm}^{-3}$ ) and one denser ( $\rho = 1.120 \text{ g cm}^{-3}$ ) than the homogeneous solution ( $\rho = 1.108 \text{ g cm}^{-3}$ ) initially in the tank. The sources at the two ends of the tank were at the same depth, 30 mm below the surface; the water depth was 150 mm and the overflow tube was located at the surface in the centre. In this case (and in many other runs) the nozzle supplying the denser source was modified so that the downward flowing plume became turbulent. The flow rate of each input was controlled to be near  $5.0 \text{ ml min}^{-1}$ . In this case, only the refractive index of the samples was determined (since it was the simpler property to measure), and the density structure at the central section was deduced from this as a function of time.

Figure 3 is a plot of the evolution of the densities of samples from the bottom of the tank, and at the top, as represented by the overflow. It is seen that both of these evolved slowly from the initial density in the tank until a substantial vertical gradient had been established. The bottom density increased monotonically by the 'filling box' process until a steady state was reached at about 50 h, with a value somewhat less

Run	Tank fluid	Withdrawal	L.H. source	R.H. source
A (Control)	Salt $\rho = 1.108$	top	Salt $\rho = 1.120$ top, turbulent	Salt $\rho = 1.098$ top
B	50 : 50 mix, $\rho = 1.102$	top	Salt $\rho = 1.104$ bottom	Sugar $\rho = 1.100$ top
C	50 : 50 mix, $\rho = 1.105$	mid-depth	Salt $\rho = 1.110$ mid-depth	Sugar $\rho = 1.100$ mid-depth
D	Stratified, as at end of Run C	top and bottom	Salt $\rho = 1.110$ mid-depth	Sugar $\rho = 1.100$ mid-depth
E	50 : 50 mix, $\rho = 1.106$	top and bottom	Salt $\rho = 1.110$ mid-depth	Sugar $\rho = 1.100$ mid-depth
G	Salt $\rho = 1.117$	top	Salt $\rho = 1.121$ top, faster, turbulent	Sugar $\rho = 1.101$ top, laminar
H	50 : 50 mix, $\rho = 1.111$	top	Salt $\rho = 1.120$ top, turbulent	Sugar $\rho = 1.100$ top
I, J, K, Q (Standard)	Salt $\rho = 1.110$	top	Salt $\rho = 1.120$ top, turbulent	Sugar $\rho = 1.100$ top
M	Salt $\rho = 1.100$	mid-depth	Salt $\rho = 1.100$ mid-depth	Sugar $\rho = 1.100$ mid-depth
N	Sugar $\rho = 1.100$	mid-depth	Salt $\rho = 1.100$ mid-depth	Sugar $\rho = 1.100$ mid-depth
O	50 : 50 mix, $\rho = 1.100$	mid-depth	Salt $\rho = 1.100$ mid-depth	Sugar $\rho = 1.100$ mid-depth

S Conditions as for Run O, except that tank was 1820 mm long, depth 120 mm.

TABLE 1. Summary of the conditions used for the runs discussed. All were carried out in the 750 mm long tank (with water depth 150 mm), except for Run S, which was in a tank 1820 mm long, with water depth 120 mm.

than that of the dense input. The surface overflow density at first decreased rapidly to reach a minimum at about 3 h, reflecting the addition of less-dense solution there. As the volume of fluid added and withdrawn increased, the surface density increased again, and the final density of the overflow was equal to that of the original tank fluid, i.e. the mean density of the inputs, (which must be generally true in the steady state). Note that the mean salinity had increased, so there was an accumulation of excess salt in the tank.

Measurements of the density at mid-depth showed that this was little different from the bottom density, so the stratification consisted of a strong gradient near the surface with a weaker gradient below, as is characteristic of a turbulent filling box. Note that the final top to bottom density range lies within that of the input fluids (it is just over one third of the difference). With a single stratifying property there is no mechanism whereby the density can move outside this range. One more feature of figure 3 should be noted. The time marked 'replacement timescale' is the time needed for the two inflows to supply a volume of fluid equal to that in the tank. It is seen that the decrease in surface density and the minimum value occur well within this timescale.

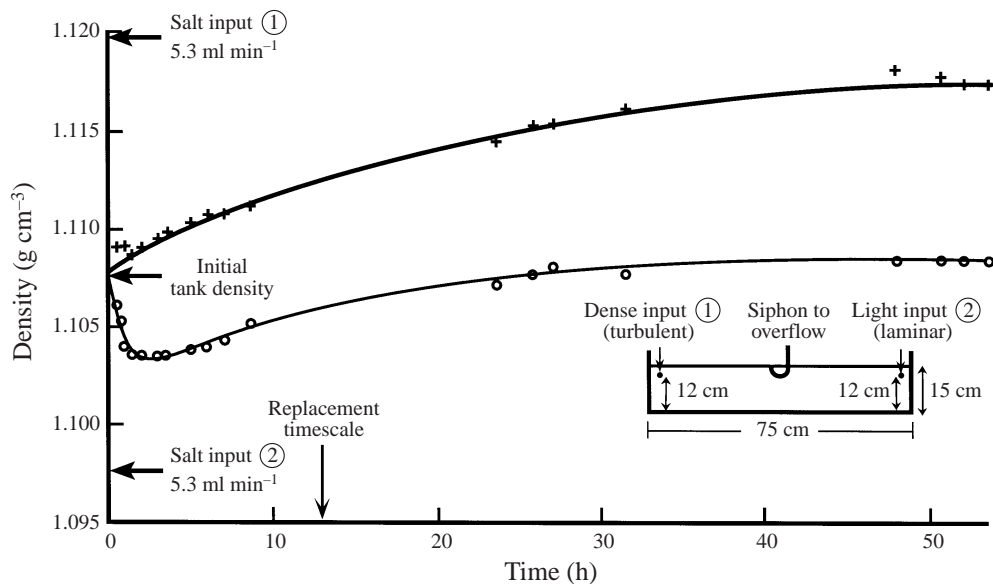


FIGURE 3. The evolution of the densities at the surface and bottom, when two sources of salt solution having different concentrations were fed at the same steady rates into the two ends of a tank filled with homogeneous salt solution of intermediate density. (Run A).

### 5. Comparison of runs starting with equal densities of tank and source fluids

In the light of the experience gained from earlier experiments (certain features of these will be presented and discussed in later sections), we asked the question: what is the simplest system which could most clearly demonstrate the principles underlying our observations, and which would best repay a more detailed and quantitative study? It was decided to concentrate on the evolution of one or more runs in as much detail and over as long a time as possible, monitoring the vertical distributions of sugar and salt until the tank achieved an asymptotic state. The simplest starting conditions we could think of were to use the same density for the two input fluids and for the initial homogeneous fluid in the tank, and to fix the inputs and withdrawal at mid-depth. The advantage of this geometry is that the system evolves to a state where there are high gradients and a sharp interface at mid-depth because of the withdrawal there, with weak stable gradients in the layers above and below. Thus fewer samples are needed to characterize the overall vertical structure.

In the series of experiments described in this section three runs were compared, differing only in the initial fluid in the 750 mm long tank: pure salt solution in run M, pure sugar solution in Run N and a 50 : 50 mixture of the two input fluids in Run O. The salt and sugar solutions were fed in horizontally 50 mm from each end, at equal rates close to  $5.0 \text{ ml min}^{-1}$ . Each of these experiments was monitored for over a week, covering both the actively convecting and rundown states, and samples were withdrawn at frequent but irregular intervals. The sampling positions were generally at 150 mm from each end of the tank, and at each of these, samples were withdrawn from the bottom and heights above the bottom of 30 mm, 65 mm (10 mm below the interface which developed at mid-depth), 85 mm (10 mm above the interface), 130 mm and (for Runs N and O) also at the surface. For each sample the density and refractive index were measured, and the salt and sugar concentrations deduced as described in

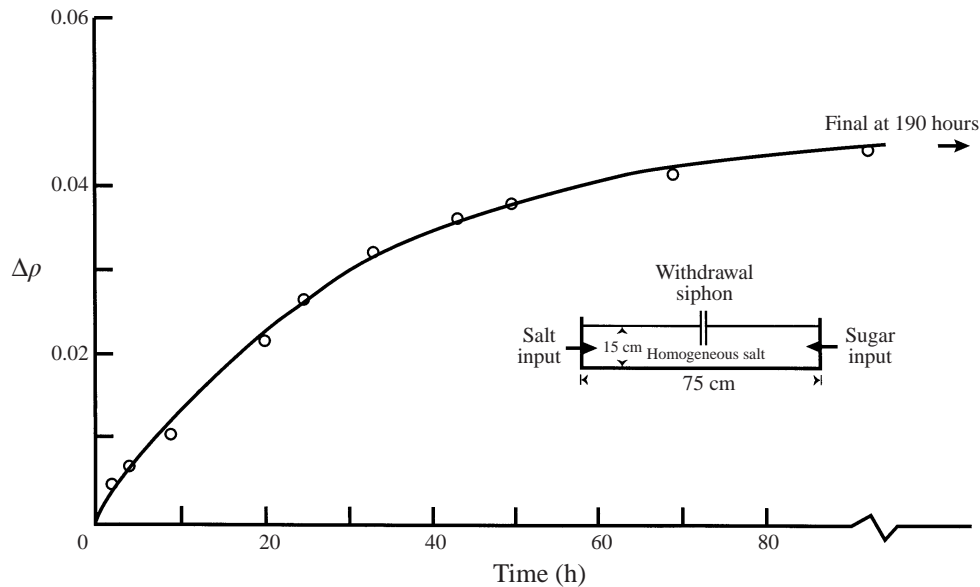


FIGURE 4. The density difference ( $\text{g cm}^{-3}$ ) between the top and bottom layers in Run M (salt solution in tank initially), plotted as a function of time. The first three points represent density differences between 30 mm and 130 mm, before a central interface had developed, and the others used the samples at 65 mm and 85 mm.

§3. Notes and sketches were made of the prominent features of the flows, though no photographs were taken during these three quantitative runs.

We also carried out a further quantitative experiment (Run S) in a longer tank, again with the sources and sink at mid-depth, to provide a comparison with various features of the runs in the 750 mm tank. Run S was also continued for a long time, and observations, photographs and measurements were made in the 'final' state, although the density, salt and sugar distributions were not monitored continuously. The detailed results from Run S are described in §8.

#### 5.1. Run M. Salt solution in tank, salt and sugar inputs

Over the first 20 h in Run M the structure evolved via vertical convection (initially strong only near the sugar source, because of the large compositional contrast with the salt in the tank) followed by a complicated series of intrusions at various levels. More detailed descriptions and photographs of these intrusions in other runs will be presented in §§6 and 7. At no stage were thin persistent layers observed near the top and bottom boundaries (in contrast to Runs N and O, discussed below), but since no surface samples were taken in Run M we do not have a direct measure of the density there. (The samples in Run M were evidently withdrawn from smooth transition regions, rather than from within or outside distinct boundary layers, as measured in the other two runs.) The system evolved to a state in which there was a clear central interface, and the simplest and most straightforward measure of the time history is the difference in density between the bottom and top layers. This difference is plotted in units of  $\text{g cm}^{-3}$  as a function of time in figure 4, using the samples at 30 mm and 130 mm (taken near the centreline of the tank) for the first 20 h and those at 65 mm and 85 mm (the mean of the values at the two ends of the tank) thereafter, once the central interface had become established. The density difference increased smoothly



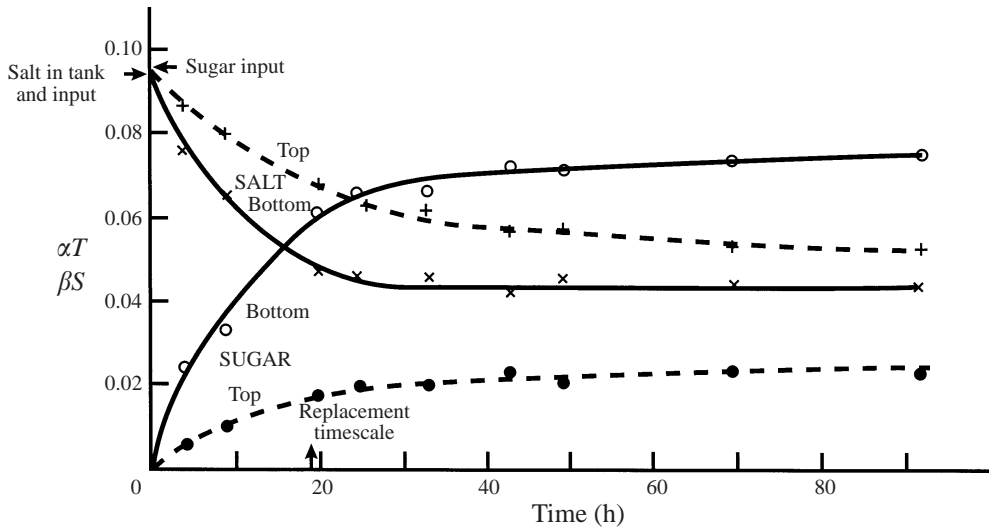


FIGURE 5. The development of the density contributions of salt ( $\alpha T$ ) and sugar ( $\beta S$ ) (both in units of  $\text{g cm}^{-3}$ ) to the densities of the top and bottom layers in Run M.

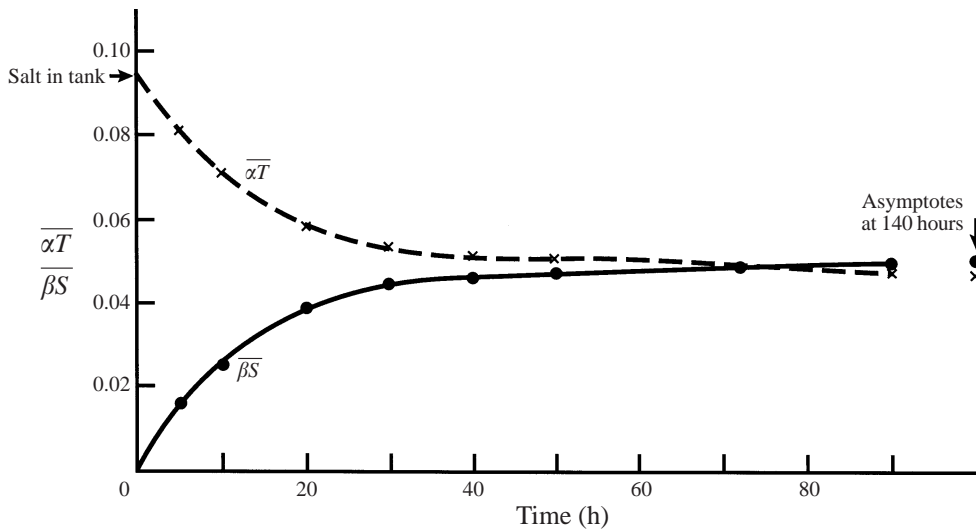


FIGURE 6. The total depth-integrated contributions of salt and sugar to the density in Run M, plotted as a function of time, in units of  $\text{g cm}^{-3}$ .

to an asymptotic value, achieved by 190 h. This behaviour is particularly striking since we began with the same fluid density in the tank and in the two sources.

The corresponding measures of the contributions of salt and sugar to the overall density difference are plotted in figure 5. (We have followed the convention that  $T$  is used to denote the property with the higher diffusivity and  $S$  that with the lower diffusivity;  $\alpha$  and  $\beta$  are the corresponding ‘coefficients of contraction’.) We have again used the mean of the values at the same heights (65 mm and 85 mm) at the two sampling positions (though there was little difference detectable between these on the scale plotted). Notice that the system evolved smoothly to a state where the sugar distribution was stable (i.e. there was a maximum in the bottom layer and a minimum

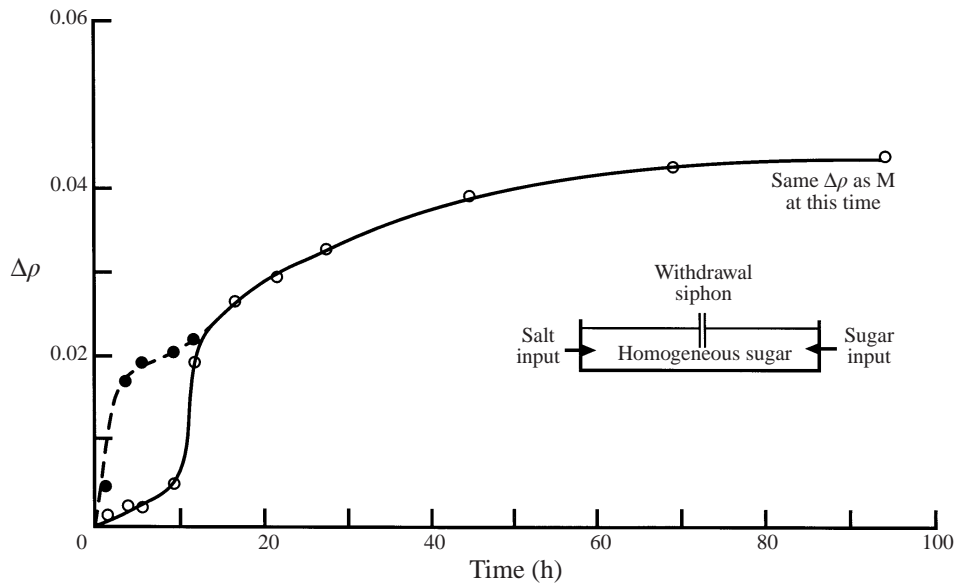


FIGURE 7. The density differences ( $\text{g cm}^{-3}$ ) in Run N (sugar solution in tank initially) between the surface and bottom of the tank (solid symbols, dashed curve) and between 30 mm and 130 mm (open symbols), plotted as functions of time.

at the top) while the salt remained weakly unstable, even in the asymptotic state. Overall, therefore, the final stratification was in the 'diffusive' sense; the implications of this will be discussed later. A check on the consistency of the measurements is provided in figure 6, in which are plotted the total depth-integrated contributions of salt and sugar to the density. Though the sugar contribution was zero at the start, in the asymptotic state the two are substantially equal, showing that in this geometry, after a long period with equal rates of salt and sugar inputs, there has been no net storage of salt.

### 5.2. Run N. Sugar in tank, salt and sugar inputs

The detailed behaviour of this run was different to that in Run M initially for two reasons: double-diffusive convection and separation were prominent near the salt source rather than the sugar source, and a thin surface layer with a diffusive interface below it developed rapidly. For the early stages of this run we have plotted both the density difference between the bottom and the surface samples and that between 30 mm and 130 mm. There is a very rapid rise in the former and a slower change in the latter compared to Run M, because of the presence of the surface layer. Comparing figure 7 with figure 4, we see that the density difference between 30 mm and 130 mm in Run N remained higher than this difference in Run M for about 90 h, but by that time it was approaching the same asymptotic value. After about 30 h, once a clear two-layer structure had developed with an interface at mid-depth, there was no significant difference in density through the two layers, between the bottom and 65 mm and between the surface and 85 mm.

The differences in the evolution can be explained qualitatively as follows; a more detailed discussion of these processes is given in §9. As the salt plume in Run N emerges from the source into an environment of sugar solution, salt diffuses out of the plume and sugar diffuses more slowly into the plume. Thus the plume will

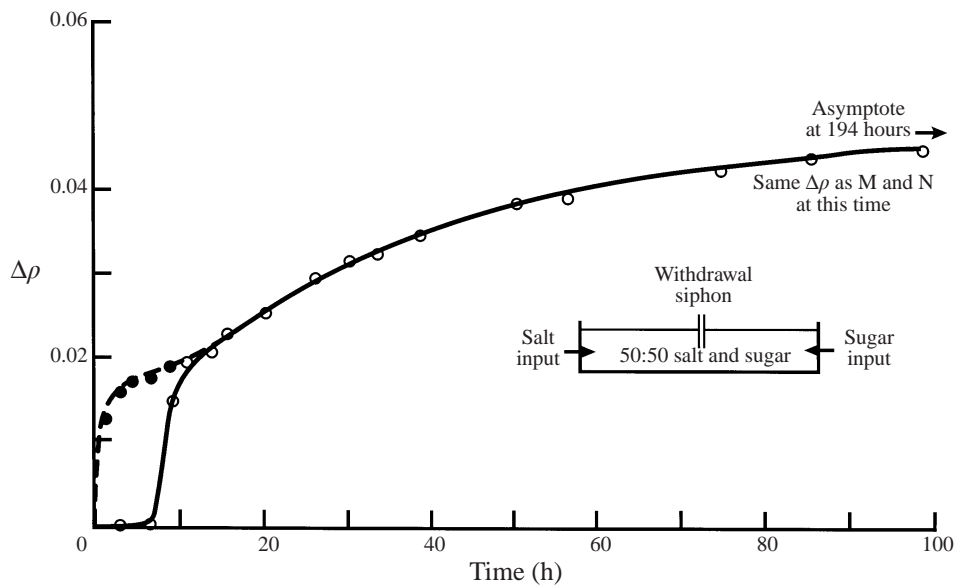


FIGURE 8. The density differences ( $\text{g cm}^{-3}$ ) in Run O (50 : 50 mixture of salt and sugar in tank) between the surface and bottom (solid symbols, dashed curve) and between 30 mm and 130 mm (open symbols), plotted as a functions of time.

become lighter and rise, while the sheath of fluid surrounding it will become denser and sink. There will be no activity at the sugar source initially because there is no compositional difference there. Similarly in Run M there will be relative diffusion across the edge of the sugar plume, so that the plume becomes denser because salt can diffuse into it from the environment faster than sugar can diffuse out, and the sheath becomes correspondingly lighter.

At first sight it appears that these processes should be antisymmetric, but otherwise equivalent. But there is an important difference in the geometry, which is not reversible. In Run N, the more rapidly diffusing salt is spreading outwards into the unconfined sheath, whereas in Run M it is diffusing inwards into the plume while sugar is diffusing out into a thinner sheath. We believe that this difference implies that the net buoyancy flux and hence the vigour of the convection will be greater in Run N. The concentrations of salt and sugar delivered initially to the top and bottom boundaries, where they form a lighter and a denser layer, will also be larger and these layers will be more stable. The rates of transport through the interfaces between the layers near the boundaries and the interior, and the net rate of change of density at the top and the bottom, will in turn be increased in Run N relative to the rates achievable by the separating sugar plume in Run M.

It was observed visually in Run N that the diffusive interface below the surface layer moved downwards through the course of the experiment as more salt-rich fluid was supplied to this layer by the plume, and this sharp interface persisted until eventually it became the interface at mid-depth separating the upper and lower layers. The density of the surface layer decreased faster than the density at the bottom increased, and its sugar concentration also fell rapidly from the initial value in the tank, because little sugar was transported with the salt plume into this layer. We have not reproduced the plots of the overall evolution of sugar and salt for Run N; the asymptotic structure was however very close to that shown in figure 5, with a

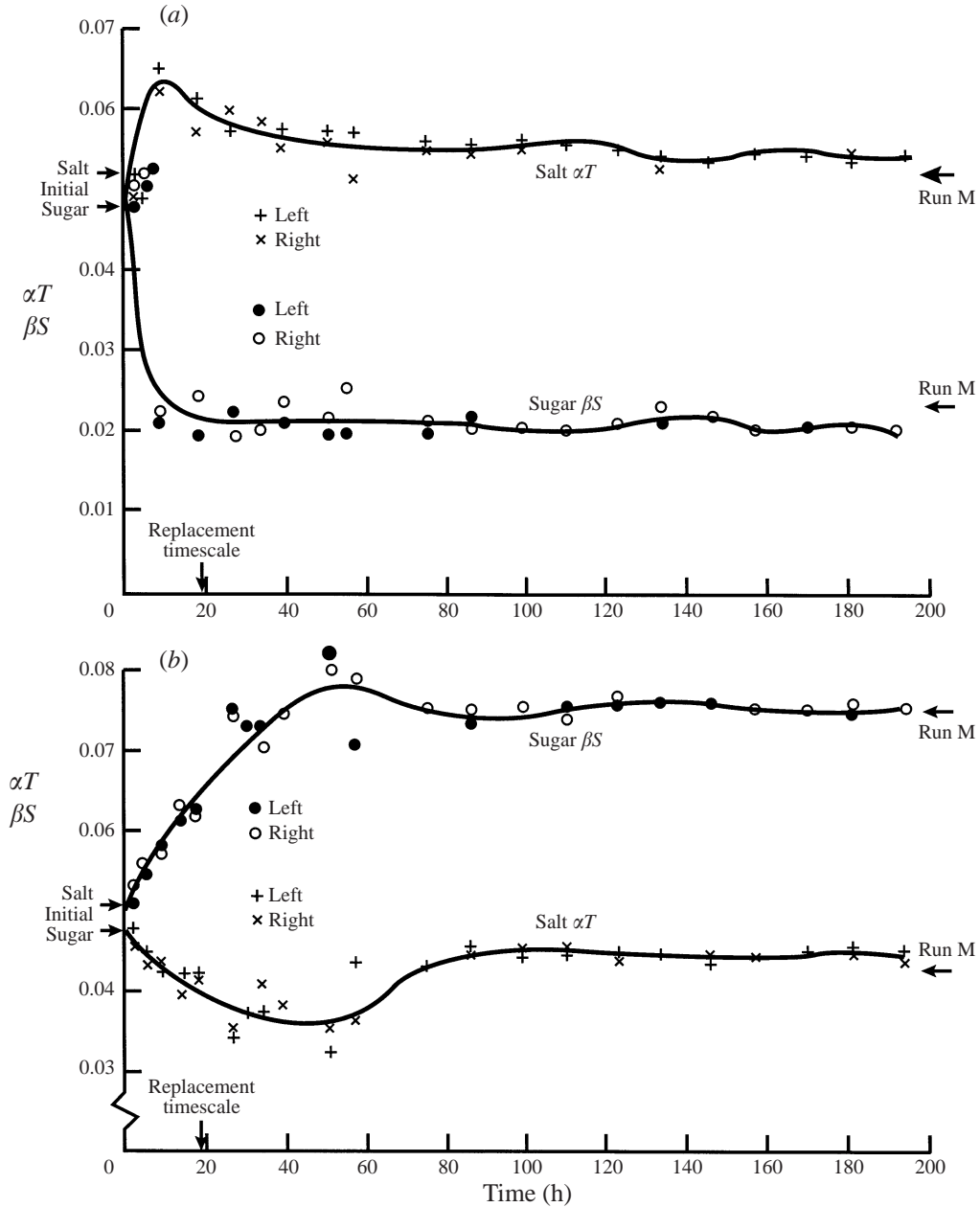


FIGURE 9. The separate contributions of salt ( $\alpha T$ ) and sugar ( $\beta S$ ) (in units of  $\text{g cm}^{-3}$ ) to the densities of the two layers in Run O: (a) top layer; (b) bottom layer. The corresponding asymptotic values for Run M are marked on the right.

stable overall sugar distribution and weakly unstable salinity. The approach to this state was also very different from that in Run M, since the sugar concentration in the lower half of the tank needed to change little to achieve the final value in Run N while in Run M it had to increase from zero to reach the same concentration. More detailed measurements will be plotted for Run O, and the mechanisms whereby the final state was achieved are discussed later.

Time (h)	75	86	99	110	123	134	146	157	170	181	194	219
L.H. samples	33	35	37	39	41	43	45	47	49	51	53	55
R.H. samples	34	36	38	40	42	44	46	48	50	52	54	56

TABLE 2. The identifying numbers for the data plotted in figures 10 and 11. The samples were withdrawn at the times shown (to the nearest hour).

### 5.3. Run O. 50 : 50 mixture of salt and sugar in tank, salt and sugar inputs

As shown in figure 8, the initial rate of change of the density difference between top and bottom of the tank was greater in the early stages of Run O than in either of the two previous runs, probably because double-diffusive convection was generated immediately near both sources. Both the extreme difference and that between 30 mm and 130 mm are plotted up to 11 h, but only the latter (the mean between the two ends of the tank) for the rest of the run. This difference remained small up to 7 h, and then increased rapidly as the surface and bottom interfaces passed these levels. The density difference then remained higher than that in Run M for 30 h, but after that the overall evolution of Run M and Run O was closely the same.

In figure 9 the separate contributions of salt and sugar to the densities of the two layers are plotted (using expanded scales compared to that for Run M, as plotted in figure 5). Figure 9(a) plots the values in the top layer and figure 9(b) those in the bottom layer; both left and right samples are shown, and this run was followed in detail for about twice as long as the previous two. There is considerably more scatter in the individual contributions than there is in the mean density, because of the sampling of salt-rich or sugar-rich intrusions which happened to be passing the sampling points when fluid was withdrawn. Note that all the concentrations had to change less to achieve the final state than they did in the other two runs but that they overshoot their asymptotic values, before settling back and becoming quasi-steady. There are small continuing oscillations about the asymptotic values, which again are close to those achieved in Run M; the fluctuations may be due in part to differences in the concentration of the source fluids, which were replenished many times during this run, and to small unmonitored variations in the input pumping rates.

We will now look in more detail at the vertical structure at the two ends of the tank in Run O, by plotting the salt and sugar concentration data within each layer on  $\Delta\alpha T$ ,  $\Delta\beta S$  diagrams, i.e. the axes represent the contributions of salt and sugar to the vertical density gradient. For the lower layer the differences between the values at 30 mm and 65 mm, and for the upper layer the differences between 85 mm and 130 mm, have been used as measures of the vertical gradients in the layers. (These are very much smaller than the overall property differences between the top and bottom layers, which are shown in figures 5 and 9.) Only the measurements made after 75 h have been plotted, in order to concentrate on the quasi-steady behaviour, rather than the earlier period during which large fluctuations were recorded (as shown in figure 9). The analyses of samples from the left of the tank, closer to the salt source, are shown in figure 10, and the corresponding measurements for the samples from the right of the tank, closer to the sugar source, in figure 11. The identifying numbers of the sets of samples, and the times at which they were taken, are set out in table 2; the odd-numbered samples were those from the left of the tank, and the even-numbered samples those from the right.

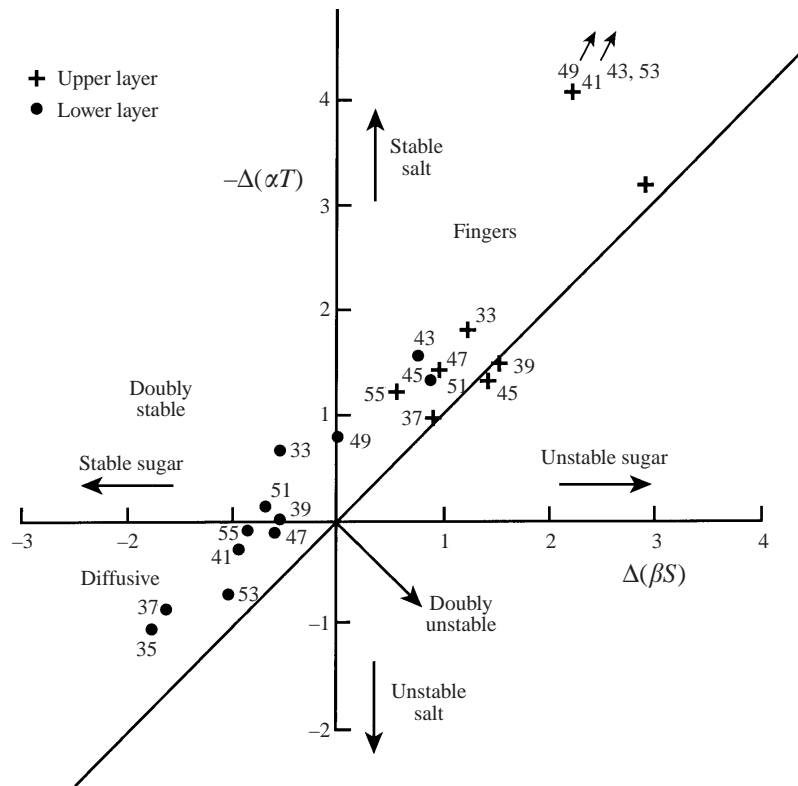


FIGURE 10. The evolution of the vertical density differences due to salt and sugar in the upper and lower layers in Run O, measured at the left of the tank, near the salt source. Differences between samples at 85 mm and 130 mm and between 30 mm and 65 mm above the bottom have been used as measures of the vertical gradients. This plot on a  $\Delta\alpha T$ ,  $\Delta\beta S$  diagram has the areas marked corresponding to regions where fingers or 'diffusive' convection are possible, and the numbers against the points correspond to the times recorded in table 2. (Unit:  $10^{-3} \text{ g cm}^{-3}$ .)

The left hand samples (figure 10) are consistent with a salinity maximum at the level of the interface, with sugar concentrations increasing away from this, both upwards and downwards. Thus there is a predominantly diffusive stratification in the lower layer, and fingers in the upper layer – but there are transient exceptions, with fingers occasionally detected in the lower layer, as well as some periods with both properties stable. On the right of the tank, however, (figure 11) there are predominantly fingers at all times in both the upper and lower layers, with occasional measurements showing doubly stable and weakly unstable stratification. Thus not only is sugar moving out along the interface, but it is also being convected upwards towards the surface. Fingers dominate the double-diffusive transports in the whole of the upper layer, as well as in the right-hand quadrant of the lower layer.

These observations suggest that in Run O, carried out in a tank 750 mm long, the dynamic interactions between the two sources, through the passage of intrusions across the whole tank, remained important throughout. In other words, in the quasi-steady asymptotic state the vertical structure within each layer was not dominated by one-dimensional double-diffusive convection corresponding to the local properties of the fluid near the central interface. Near the sugar source, the structure did not consist of diffusive layers above the interface and fingers below, but it was evidently

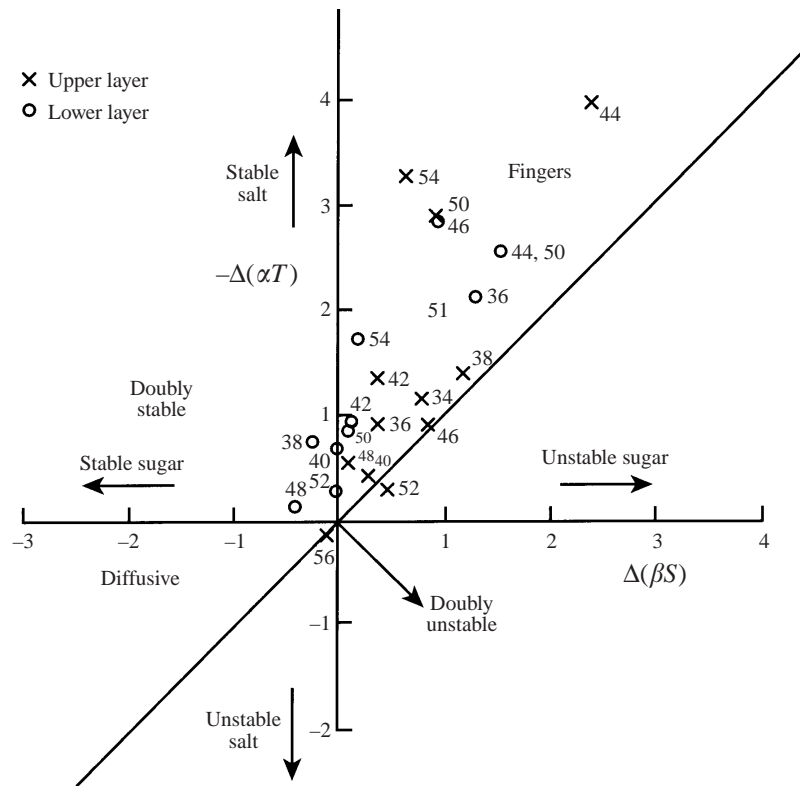


FIGURE 11. The corresponding plot to figure 10, but at the right-hand end of the tank, near the sugar source.

responding to the advection of salt from the other end of the tank. The behaviour is different in a longer tank, as discussed in § 8.

## 6. Effects of varying the input geometry and the initial conditions

### 6.1. Bottom salt input and top sugar input, mixed solution in tank

The next example, Run B, has been chosen to emphasize again the very different behaviour associated with double diffusion, under conditions similar to the 'control' experiment described in § 4. A series of photographs of the intrusions that are an essential feature of the evolution was also taken in this run. The sugar source was at 120 mm above the bottom and the overflow near the surface (at 147 mm in a depth of 155 mm), while the salt source at the other end of the tank was 30 mm above the bottom. The densities of the inputs were  $\rho = 1.104 \text{ g cm}^{-3}$  for the salt and  $\rho = 1.100 \text{ g cm}^{-3}$  for the sugar source. The tank was filled with a 50 : 50 mixture of the two input solutions, so that the convection near both sources was double-diffusive from the start. The flow rates differed a little from the nominal value of  $5.0 \text{ ml min}^{-1}$ , the measured values being  $5.20 \text{ ml min}^{-1}$  for salt and  $4.75 \text{ ml min}^{-1}$  for sugar.

Figure 12 is a plot of the overflow and bottom densities near the centre of the tank as a function of time. There was an initial rapid increase in the density at the bottom, followed by a monotonic increase at a decreasing rate until an asymptotic value was approached after about 50 h. Note that this density is much larger than that of the input salt solution, as a result of double diffusion. The surface density decreased slowly

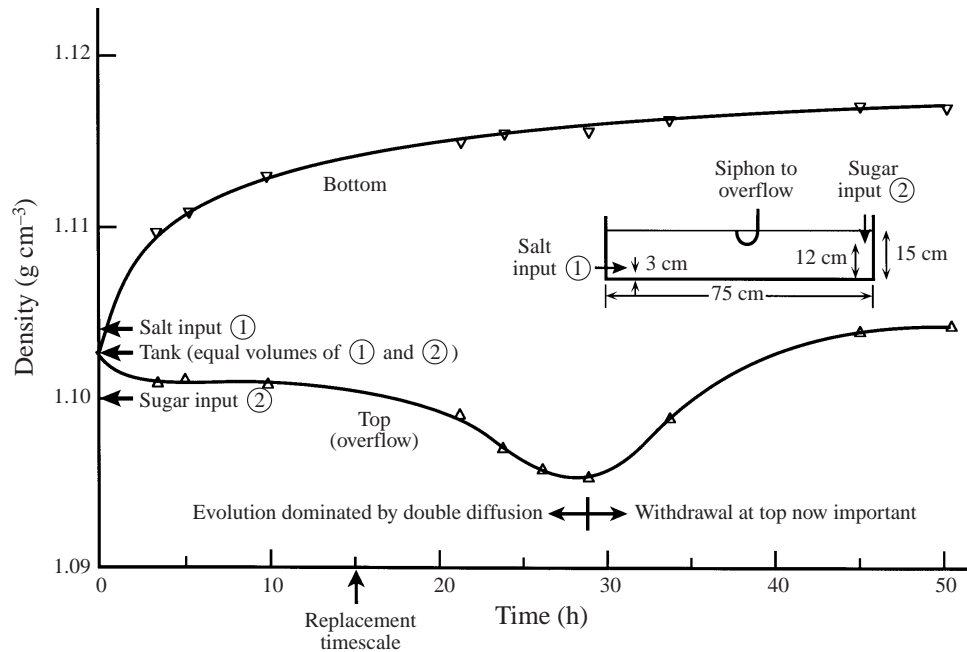


FIGURE 12. The evolution of the density structure when a less-dense sugar solution was fed in at the top, and a denser salt solution at the bottom, of a tank initially filled with a 50 : 50 mixture of the two input fluids. Double-diffusive effects are important, and the final vertical density contrast is much larger than that of the inputs. (Run B.)

during the first replacement timescale, then it decreased more rapidly as a result of the vertical double-diffusive transports and reached a minimum at about two replacement timescales. After that the overflow density increased again as the surface withdrawal became more important. The final density of the overflow was approximately the mean of the two inputs, which, as suggested above, must be generally true of the steady state. The total vertical density difference at the end of the experiment was  $0.013 \text{ g cm}^{-3}$ , approximately 3.2 times that between the salt and sugar inputs, and at an intermediate time it reached  $0.021 \text{ g cm}^{-3}$ . This is a very different behaviour from that observed with the two salinity sources, without double diffusion. Note, however, that with surface withdrawal it is possible to achieve only half the overall density difference measured in the runs with mid-depth withdrawal, discussed in § 5. In both cases the mean density of the overflow must match the mean of the inputs, but with surface withdrawal half the potentially stratified region is effectively removed.

The influence of double diffusion in producing the observed evolution of density plotted in figure 12 can be better understood by examining the series of photographs taken at various stages of this experiment (figure 13). After 2 h (figure 13*a*) sugar was still feeding in at the top and salt at the bottom of the tank, with strong double-diffusive convection forming plumes which extended through the depth in each case. The distortion of dye streaks shows that a stable stratification had already been set up. After 6 h (figure 13*b*) both inputs were initially flowing horizontally into the tank. Note that at the level of the salt source there was a sharp interface with plumes rising and falling away from it. The more rapid diffusion of salt into the plume produced by the sugar source, compared with the rate of diffusion of sugar out of it, caused this inflow to become denser, so that it was deflected downwards and extended to the



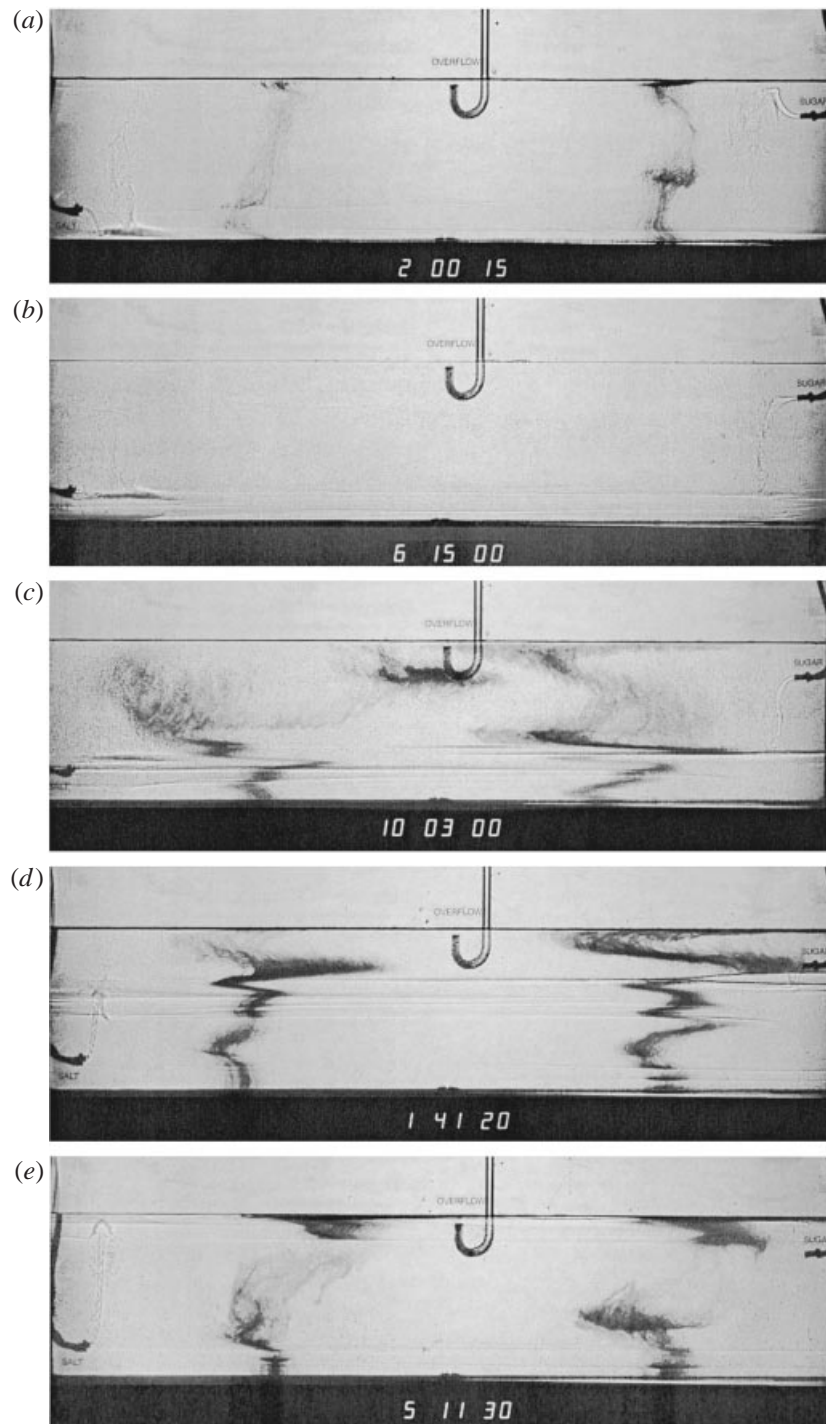


FIGURE 13. Photographs taken during Run B at the times shown on the clock (hr min sec) in each frame. (Note that the 10h figure is missing on frames (d) and (e), which should read 21 41 20 and 45 11 30 respectively.) A detailed interpretation of various features, and their relation to the evolution of the densities shown in figure 12, is given in the text.

lower interface. The surrounding fluid is less visible, but it must have become lighter and relatively sugar-rich, and convected upward.

Figure 13(c), taken after 10 h, shows the further development of the dense bottom layer, with several diffusive interfaces above it. Most of the inflow from both sources was at this time spreading into the tank about one third of the depth above the bottom. The separation of the sugar plume near the source had evidently continued to feed an excess of sugar to the top of the tank, since fingers were prominent over the top two-thirds of the tank. The strong upward convection above the salt source was followed by downward transport by fingers and a horizontal outflow to the right. By 21 h 41 min (figure 13d) the vertical density gradient had evolved considerably, so that the sugar source fluid was denser than that at the top of the tank and the salt source less dense than the tank fluid at the input level. As a result, the major volume flux from both inputs flowed out at levels near one third of the depth from the top of the tank. At this time there was a complex series of interleaving layers and interfaces, with evidence of both diffusive interfaces and salt fingering. Finally, after 45 h (figure 13e), both inputs were much less dense than the evolved tank fluid, and were feeding in near the top of the tank. The convection at mid-depth indicates that the gradient was weak there.

#### 6.2. *Runs with the same input and withdrawal rates, different initial conditions*

Another question of relevance to the ocean is the following: are the properties of the inflows and outflows from a region sufficient to determine the asymptotic state, or can the initial stratification also have an influence? This can be examined by comparing two runs in our series, which had the same geometry and composition of the two sources, but different initial conditions in the tank.

Both of these, Runs D and E, had inputs of salt solution  $\rho = 1.110 \text{ g cm}^{-3}$  and sugar  $\rho = 1.100 \text{ g cm}^{-3}$  flowing in at mid-depth at opposite ends of the tank, with equal flow rates  $5.0 \text{ ml min}^{-1}$ . In order to eliminate the sharp interface at mid-depth due to placing the withdrawal there also, two withdrawal tubes were inserted, at the top and bottom in the centre of the tank. The bottom tube was pumped out at  $5.0 \text{ ml min}^{-1}$ , and the top was allowed to overflow through a constant-head device at the same rate. Run D was a continuation of C, which will not be described in detail here; it was similar to Run O except that the input densities of sugar and salt were not equal. Run C had evolved to a nearly steady state over five days from a homogeneous 50 : 50 mixture of the input fluids, using a mid-depth withdrawal. When the top and bottom withdrawal geometry was substituted for this, the vertical density difference fell from the value of  $0.044 \text{ g cm}^{-3}$  reached at the end of Run C to a steady value for Run D of  $0.033 \text{ g cm}^{-3}$  in 54 h, as the central interface thickened and fluid was drawn off from the top and bottom.

Run E, on the other hand, was started with a homogeneous 50 : 50 mixture of the input fluids and top and bottom withdrawal from the beginning. Both inputs were immediately double-diffusive, with the sugar plume rising to the top of the tank and the salt plume falling to the bottom, followed in each case by strong convection, downwards and upwards respectively. After three hours, layers about 10 mm thick containing fingers had developed at the top and bottom boundaries, and the density difference between the two overflows was  $0.012 \text{ g cm}^{-3}$ . At five hours these layers had doubled their thickness, and weak diffusive interfaces had appeared in the centre of the tank, but otherwise the structure was little changed. At that time the density difference had evolved to  $0.014 \text{ g cm}^{-3}$ ; the appearance and densities had changed little at 22 h, so this can be taken as the steady state, achieved much more rapidly

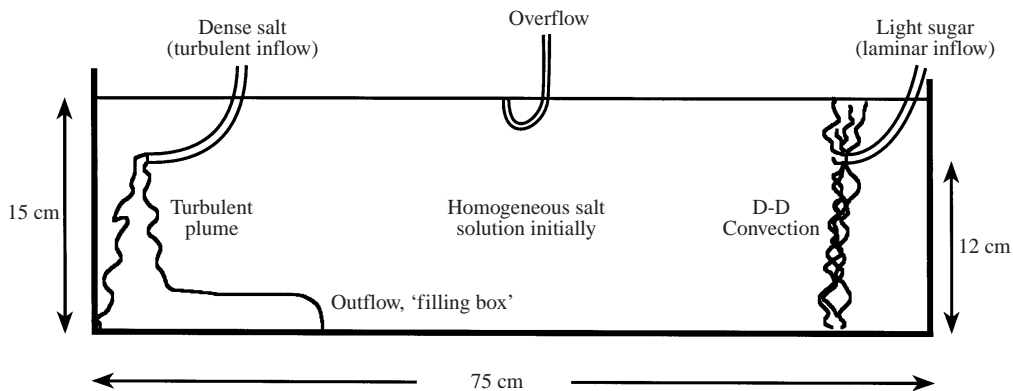


FIGURE 14. The input conditions for Runs I, J, K and Q, which were monitored in detail using different techniques in the nominally identical experiments.

than in the previous experiment. Run E could not evolve to a state with as large a vertical density difference as run D, because the lightest and densest fluids were continually being withdrawn from the region, before double diffusion could achieve its full effect. Clearly the initial stratification had a significant influence on the progress of these two runs.

## 7. Series of related runs: multiple measuring techniques

As the results of early experiments became available, it was apparent that more detailed and quantitative measurements of various kinds were needed. The next experiments to be described are a series of runs in a geometry like that described in §4 for Run A, the 'control' experiment (see figure 14). The experiments were nominally identical, but different properties were measured in each run. The inputs and withdrawal were again at the top, but now the less-dense laminar input was sugar solution, while the denser turbulent input was salt and the tank was filled with homogeneous salt solution. The time history of the input plumes and the resulting intrusions were followed using dye streaks, with still photographs and time-lapse video recording. Vertical profiles of density and refractive index were deduced by withdrawing samples, and the corresponding contributions of salt and sugar to the density calculated for each sample. A continuous record of the sugar concentration through the width of the tank at several sections was obtained using a polarimeter; this provided a non-invasive means of monitoring the variability due to the passage of intrusions along the tank.

### 7.1. Observations of dye streaks

Figure 15 shows the early stages of an experiment, Run G, having salt  $\rho = 1.117 \text{ g cm}^{-3}$  in the tank, with an input of sugar  $\rho = 1.101 \text{ g cm}^{-3}$  at a rate of  $5.0 \text{ ml min}^{-1}$  and salt  $\rho = 1.121 \text{ g cm}^{-3}$  at  $20.3 \text{ ml min}^{-1}$ . (This run was selected for illustration because the photographs are the best available, though the larger rate of input of salt was not that adopted for the other 'standard' runs.) After 4 min (figure 15a) the distortion of the dye streak near the salt plume shows that the behaviour there is like a one-component 'filling box', without any double-diffusive effects. There is already strong convection and separation near the sugar plume, however, because of the large property differences which have been introduced. Figure 15(b), taken at

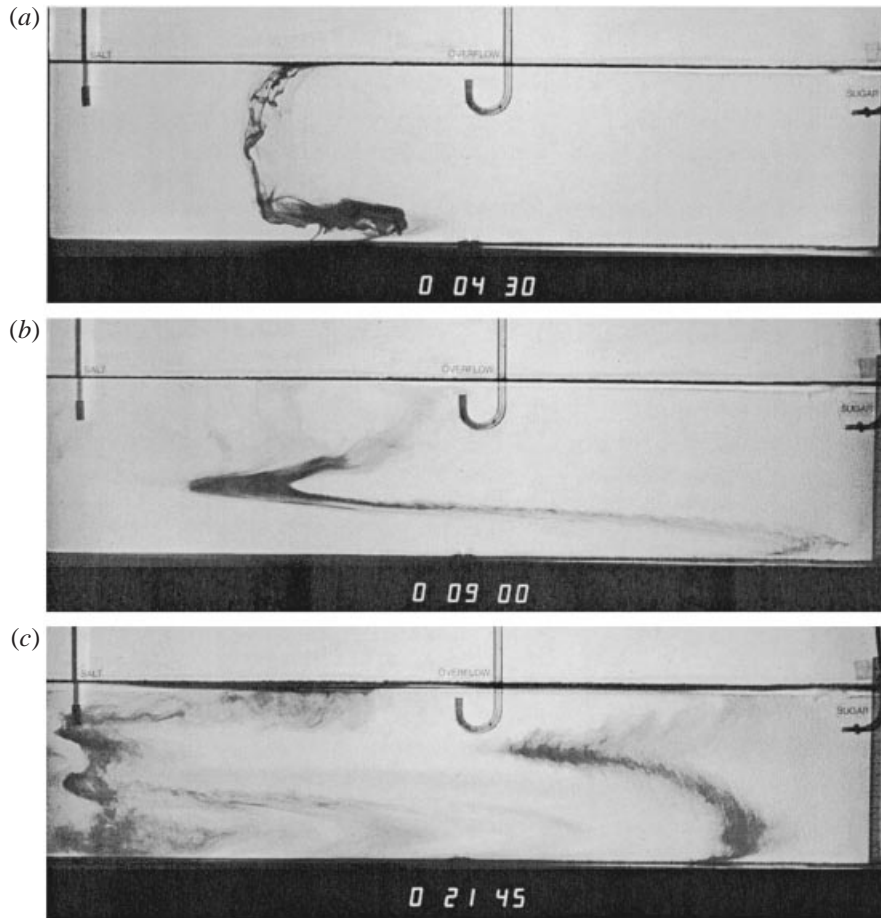


FIGURE 15. The early stages of an experiment (Run G) in which a denser, turbulent source of salt and a less-dense, laminar source of sugar fed into a tank of salt solution. The salt outflow along the bottom is not double-diffusive, whereas the sugar intrusion above this exhibits strong double-diffusive effects. The features of note at the three times are discussed in the text.

9 min, shows the bottom salty current continuing to spread across the bottom, with a counterflowing sugar-rich intrusion above it supplied by the downward convection near the sugar source. The fact that this is spreading at a shallower depth implies that the buoyancy flux is less than that of the salt plume. Figure 15(c), taken 2 min 45 s after two more dye streaks were added, shows the further development of this flow. Note the rise in the level of the sugar intrusion due to the change in density profile produced by the 'filling box' fed by the salt plume, and the fingers forming at the interface below the sugar-rich intrusion.

This third stage provides a simple analogue of the spread of water from a marginal sea, at an intermediate level in the density gradient set up by the source of bottom water. More specifically, the salt plume can be thought of as Antarctic Bottom Water, and the sugar intrusion as the Mediterranean Outflow, equivalent to a hot salty intrusion with fingers below, as is observed in the oceanic case.

The later stages of a 'standard' experiment, Run I (after about a day – the 10 h figure is missing on the clock) are shown in the photographs of figure 16. The salt in

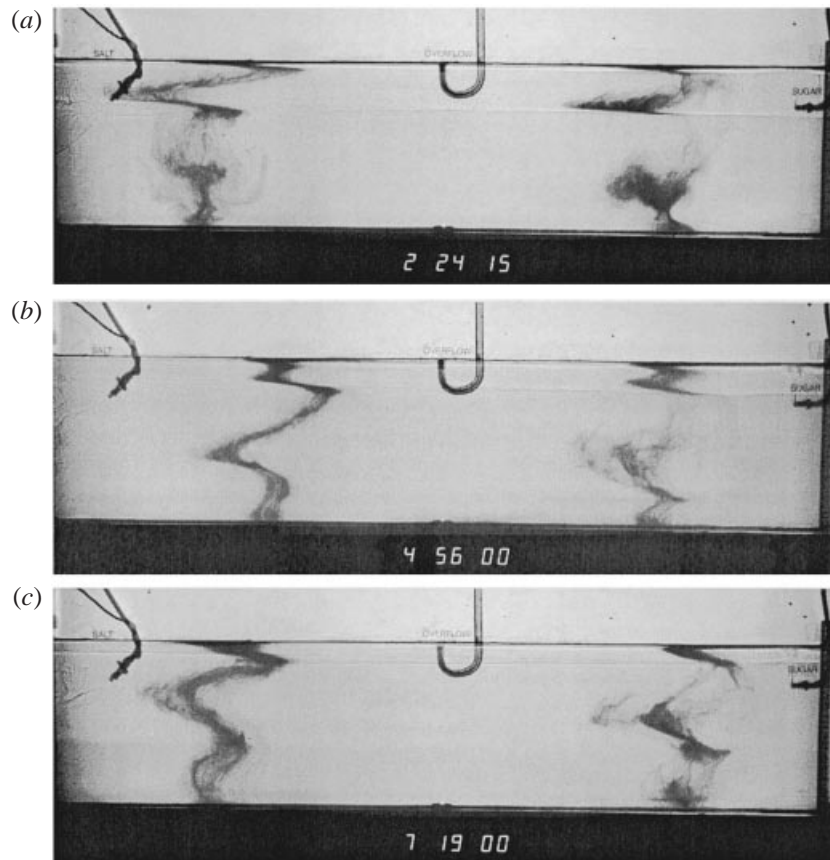


FIGURE 16. The later stages of a 'standard' experiment (Run I) after about a day. (Note again that the 10 h figure is missing on the clock.) (a) At 22 h 24 min there was a strong interface and shears at the top, and the salt plume was penetrating to about mid-depth. (b) At 24 h 56 min and (c) at 27 h 19 min there was a steady rise of the outflows of both the salt plume and intruding sugar-rich flows.

the tank had  $\rho = 1.110 \text{ g cm}^{-3}$ , the turbulent salt source  $\rho = 1.120 \text{ g cm}^{-3}$  and flow rate  $5.3 \text{ ml min}^{-1}$ , and the laminar sugar source  $\rho = 1.100 \text{ g cm}^{-3}$  and rate  $4.8 \text{ ml min}^{-1}$ . The dye streaks put in at the beginning of the experiment had faded by this time, and new dye was added at the left and right 1 min before each photograph was taken. Figure 16(a), at 22 h 24 min, shows a prominent interface and strong shears at the top, and slower motions at the bottom. At this time the salt plume was penetrating to about half the depth of the tank. At 24 h 56 min and 27 h 19 min (figure 16b, c) the salt plume was feeding out at increasingly higher levels and the intruding flows away from the sugar input had risen too. This behaviour will be described and explained in more detail later, for another run.

### 7.2. Polarimeter measurements of sugar concentrations

The observations of dye streaks just described raised a question which could only be resolved using a different technique. What was seen using the dye were the features which happened to be marked when the dye was added, at rather arbitrary intervals during an experiment. Overnight, no observations were made at all in long-running experiments, and so it may well be asked: how representative are

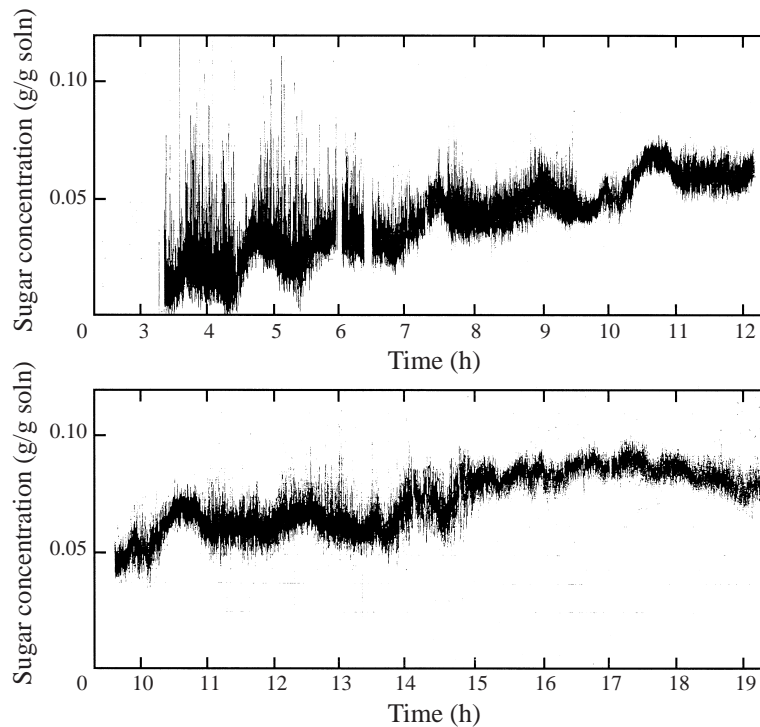


FIGURE 17. Reproduction of the output from a recording polarimeter with the beam on the centreline of the tank; a calibrated scale of sugar concentration has been added. There was a general rise in the sugar concentration over time, with superimposed fluctuations on two timescales. The short-period oscillations are due to sugar/salt fingers, and the longer periods are caused by the passage of fronts.

the visual observations? To obtain a long continuous record of the intrusions and their variability, the recording polarimeter developed by Dr B. R. Ruddick (personal communication 1978) was used. A beam of polarized light was shone through the tank; the instrument locked on to the plane of polarization of the emerging beam and gave a voltage reading proportional to the angle of rotation, and hence to the total amount of sugar in the path.

Figure 17 is such a record obtained in a standard run (Run Q), on the centreline and 58 mm above the bottom of the tank. There was a general rise in the sugar concentration as sugar was added to the tank. Superimposed on this trend were two kinds of variability: short-period fluctuations of high amplitude which are attributed to sugar/salt fingers in the beam, and longer-period oscillations which are due to the arrival of intrusions or fronts at the measuring position. The latter had a characteristic timescale of 45–60 min. Thus although the mean vertical profiles of density and salt and sugar concentrations seemed to have reached an asymptotic state by the end of this run, the intruding motions were still being actively driven and so the ‘final’ state was at best quasi-steady.

### 7.3. Measurements using time-lapse video

The rise in the level at which the salt plume fed into the body of the tank, noted above, was another puzzling feature which required continuous observations for its resolution. A long record was obtained in standard Run K using a time-lapse video recorder, and various features were measured during playback. Figure 18 is a plot of

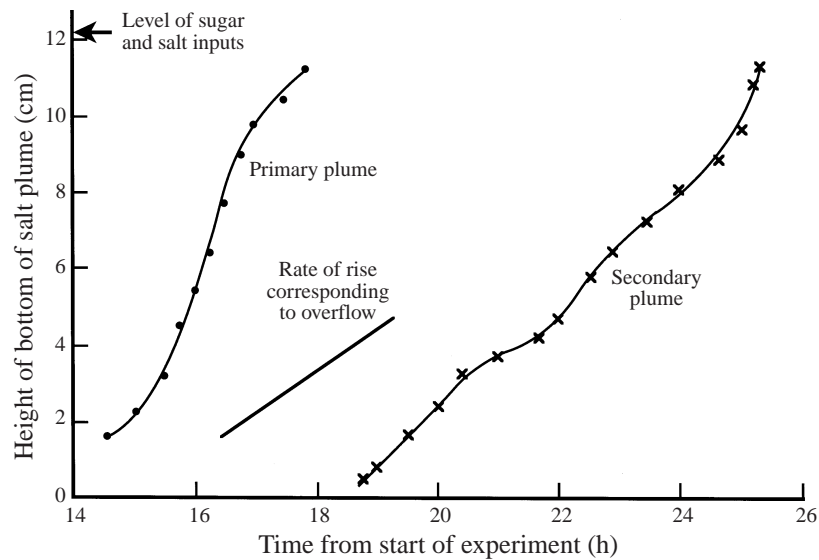


FIGURE 18. The height of outflow of the salt plume into the environment in Run K, monitored using time-lapse video. Between 15 and 25 h into the experiment this gradually rose from the bottom to the surface, dropped rapidly, then rose again. The reasons for this behaviour are discussed in the text.

the level of salt plume outflow into the interior. As observed in the still photographs for Run I this rose steadily from near the bottom to the surface in a period of just under 4 h, much faster than could be accounted for by the filling-box mechanism. Then, surprisingly, it plunged to the bottom and a secondary plume rose again to the surface, rather more slowly than the first time. This must be explained in terms of the evolving density structure, together with the double-diffusive nature of the stratification.

A detailed rationalization of this behaviour has been given by Dr E. C. Carmack (personal communication) and the following is based on his suggestions. Briefly, the first rise of the salt inflow was due to its being lifted by an undercurrent of sugar-rich fluid of increasing density flowing along the bottom from the right. This lifting was aided by a decrease in density of the salt-rich layer due to double-diffusive transports through the interface below it, together with some mixing with the surface layer, which over this period was lighter than the original tank fluid. When the salt plume reached the surface neither of these mechanisms for decreasing the density of the outflow could operate; the salt input was again denser than the fluid below it in the tank and it sank to the bottom. The second rise sequence proceeded in the same way, but by the time the outflow had risen to the surface again there was a general increase in density which prevented a further cycle.

#### 7.4. Analysis of withdrawn samples

The most detailed measurements made in this series of experiments were those using samples taken at various depths and times. The density and refractive index of each sample were used to calculate the separate contributions of salt and sugar to the density, as described above, and hence to determine the evolving double-diffusive state of the system. The procedure was tedious and time-consuming, so a full coverage of

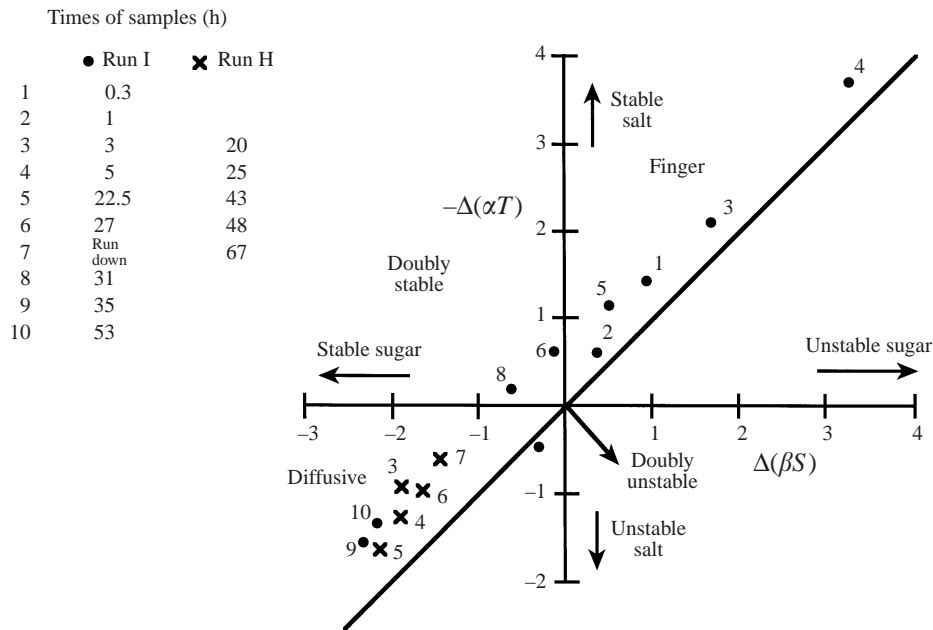


FIGURE 19. The evolution of the density differences due to salt and sugar between mid-depth and the bottom of the tank, measured on the centreline in Runs H and I. This plot on a  $\Delta\alpha T$ ,  $\Delta\beta S$  diagram, with the areas marked corresponding to regions where fingers or 'diffusive' convection are possible, shows that the stratification began in the finger sense but had changed to the diffusive sense by the end of the experiment. (Unit:  $10^{-3} \text{ g cm}^{-3}$ .)

the tank in space and time was out of the question, and only a few positions could be chosen for study in each run.

In standard Run I, samples were withdrawn and analysed from the overflow, from the top, mid-depth and bottom at the centre of the tank, and also from the bottom at each end. On analysis, the most striking overall indicator of the nature of the evolution was the difference between the salt concentrations at the bottom and mid-depth and the corresponding difference for sugar, both expressed in terms of their contributions to the local density gradient in the lower half of the tank.

Figure 19 shows these measurements, made at various times, plotted on a  $\Delta\alpha T$ ,  $\Delta\beta S$  diagram. The areas corresponding to doubly stable or doubly unstable gradients, and those where fingers or 'diffusive' convection are possible, are marked. Note that results have also been included for the later stages of Run H, which began with a 50:50 mixture of salt and sugar in the tank, and the same input conditions; it later evolved to a state similar to Run I, and continued longer.

Initially, and for nearly a day, the stratification was in the finger sense, as is to be expected with sugar feeding in above salt solution. The points are all close to the boundary with the doubly unstable region, so that the finger convection was vigorous, but they oscillate back and forth along this boundary (as a result, it now seems clear, of the sampling of intrusions with different sugar concentrations which were passing at the time of withdrawal). At 27 h both properties were stably distributed at the central section. The sources in Run I were turned off over a weekend, so that the convection ran down; samples 7, taken just before turning the inputs on again, are not included in the plot. After another 4 h of active convection, the stratification was still doubly stable. After this time the stratification changed to the diffusive sense,



indicating that there was a dominant stable gradient of sugar at the bottom. Run H, which ran continuously, also had this distribution (from an earlier time, since there was already sugar in the bottom of the tank), and the variability in both experiments can again be attributed to the passage of fronts past the sampling position. Note that again, as in Runs M, N and O, the asymptotic state was 'diffusive'.

## 8. The effect of aspect ratio: comparison with an experiment in a long tank

In order to investigate the possible influence of the aspect ratio, after completing Runs M, N and O we carried out another experiment just like O, with the withdrawal at mid-depth but in a tank 1820 mm long and 80 mm wide. This was filled to a depth of 120 mm, so that the aspect ratio was 15, three times as large as before. The tank fluid was a 50:50 mixture of the input salt and sugar solutions, both having a nominal  $\rho = 1.100 \text{ g cm}^{-3}$  (each successive batch was made up carefully by weight, and checked with the densitometer). The inflows were also at mid-depth (60 mm), and driven by a peristaltic pump at rates close to  $5 \text{ ml min}^{-1}$ ; the combined flow, monitored by measuring the overflow volume over the whole experiment, was  $10.2 \pm 0.2 \text{ ml min}^{-1}$ .

### 8.1. Visual observations of the flow

As described for Run O in § 5, a strong double-diffusive separation occurred near both sources as soon as the inflows began, with upward and downward plumes producing a density stratification. When the tank was next observed at 19 h, prominent diffusive interfaces had formed in the bottom half of the tank at the left (near the salt source), at mid-depth in the centre (above and below the withdrawal tube) and in the top half of the tank on the right. At this time plumes from both inputs were rising to about the same level (78 mm above the bottom), with the salt plume feeding into the interior just above, and the sugar just below, a diffusive interface. The detailed layer structure changed over the next 5 h through the action of intrusions moving in from the ends, especially from the right.

At 48 h both inflows remained close to mid-depth. At the left there was a diffusive interface at 56 mm with salt flowing in on top of this, and additional diffusive layers below. Above the salt inflow there was a clear finger structure over a depth of 10 mm, with weaker fingers in the whole of the upper layer. On the right sugar flowed in under a sharp interface at 62 mm, with diffusive layers in the whole of the upper half and fingers through the lower half of the tank. There were persistent shears in each of the individual layers – the flow being to the left at the top, and to the right at the bottom of each layer, right along the tank. This general picture persisted for each of the later observations. Occasionally a new convecting layer was observed to form, to spread along the tank and then to break down. Even the 'final' state at which the photographs were taken and the samples withdrawn for analysis was still highly dynamic and actively driven by the vertical and horizontal transports.

### 8.2. Photographs of the layer and finger structure

Towards the end of this experiment, photographs were taken at each end of the tank, and sometimes in the centre, to document the characteristic structures at various times. Both the light source for the shadowgraph and the camera were moved along the tank between frames, so that there was a few minutes time gap between related pictures. The photographs in figure 20 were taken after the experiment had been running continuously for nearly a week, and just before the first set of samples

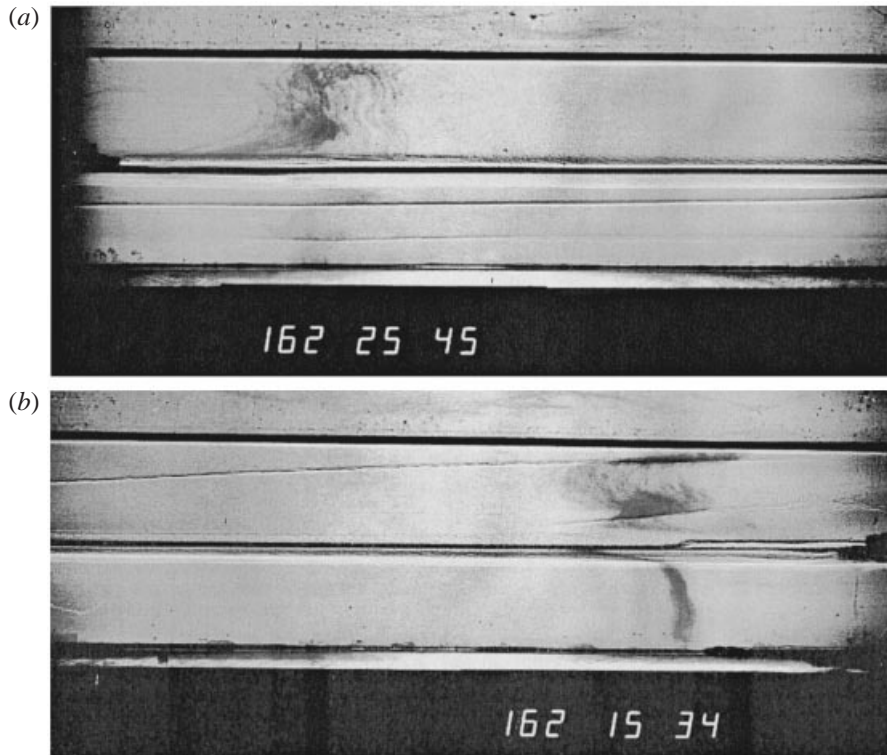


FIGURE 20. Shadowgraph pictures of the structure at the two ends of a long tank (Run S) after the experiment had been running for nearly a week: (a) taken at the left-hand end near the salt source, and (b) at the right near the sugar source. Scale: the water depth was 120 mm.

was withdrawn. In figure 20(a), at the left of the tank near the salt source, the dye streak introduced 2 min earlier shows sheared fingers in the upper half and diffusive interfaces and layers in the lower half of the tank, in which shear has rapidly dispersed the dye. Figure 20(b) shows the right-hand end of the tank (3 min after a dye streak had been added), near the sugar input which is visible as a bright layer along the top of the interface. Two diffusive interfaces, with strong shearing motions in the layer between, are seen in the upper half of the tank, while fingers with little shear occupy the lower half. The structure is antisymmetric compared with that at the other end of the tank.

At 167 h into the experiment, the input pumps were turned off and the tank allowed to 'run down'. At 283 h the pumps were turned on again, and it is of interest to record the rapid response of the tank to this reactivation. Figure 21(a) shows the left of the tank 9 minutes later with a salty intrusion moving along the interface. Already a second layer can be seen above the main intrusion, with diffusive and finger interfaces in the sense to be expected from the salt and sugar distributions. Figure 21(b), at the right of the tank, shows the corresponding, but somewhat more complicated, antisymmetric layering produced by the sugar source. (The diffusive interface visible near the middle of the upper layer was already present in the rundown state, before reactivation). Figure 21(c) shows the further development of the layer structure and the shears at the right-hand end of the tank 16 minutes later, including the formation of 'upstream wakes'.

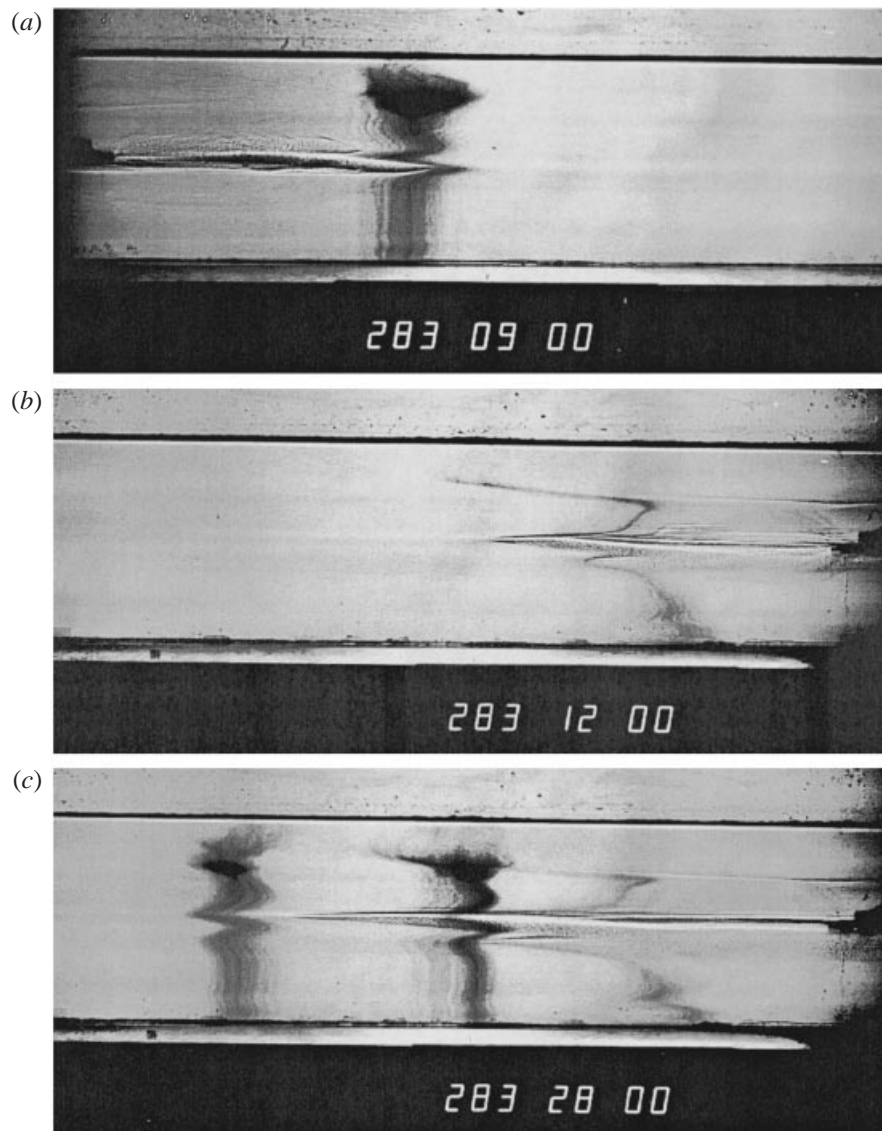


FIGURE 21. Shadowgraph pictures taken in Run S, after the experiment had been turned off for several days, and then reactivated by renewing the supplies of salt and sugar again at 283 h. (a) The salt intrusion at the left of the tank, with fingers above and a diffusive interface below; (b) the sugar intrusion on the right a few minutes later, with diffusive layers above and fingers below; and (c) a further development of the sugar intrusion.

### 8.3. Profile measurements at the two ends of the tank

As noted above, this run was not monitored continuously; instead, more detailed profiles were made at two times after the experiment had been running for many days, at 250 mm from each end of the tank. The first set of samples was withdrawn at 163 h into the experiment, just after the photos of figure 20 were taken, and a few hours before the inputs were turned off. The second set was withdrawn at 307 h, 24 h after reactivation and with the inputs still running, when it might be assumed that a

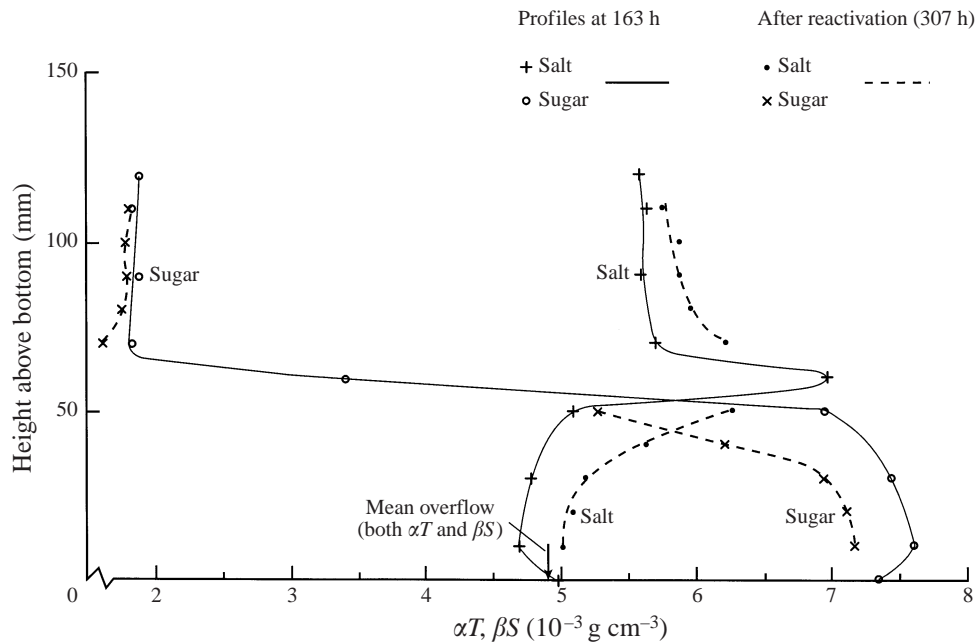


FIGURE 22. Vertical profiles of the separate contributions of salt ( $\alpha T$ ) and sugar ( $\beta S$ ) to the density, measured before the experiment in the long tank (Run S) was turned off, and after reactivation. The sampling position was 250 mm from the left-hand end of the tank, near the salt source.

new dynamic equilibrium had been achieved. The salt and sugar concentrations were deduced as before from the measurements of density and refractive index.

Since many more samples were available in this case, at fixed depths in each of the layers, the results have been plotted to show vertical profiles of the density contributions of salt and sugar separately, rather than in the simplified difference form used for figures 10 and 11 relating to Run O. Figure 22 plots the left-hand measurements, nearer the salt source, for both sets of samples, and figure 23 does the same for the right-hand samples; note that the sampling depths were different for the two sets. The structures inferred from the visual observations are now confirmed quantitatively. At the left there is a strong salty intrusion at mid-depth, with unstable salt and stable sugar distributions in the lower layer corresponding to the diffusive regime, and stable salt and weakly unstable sugar distributions in the upper layer corresponding to fingers. The mean distributions are consistent with the overall measurements plotted in figure 10 for the left-hand samples in the shorter tank. Note that in both layers the salt concentration is higher in the reactivated state.

At the right the distributions are indeed antisymmetric, corresponding to diffusive layering in the upper layer and fingers in the lower, but there is a smaller difference between the steady and reactivated states at this end. Some direct contribution to the vertical fluxes, driven by plumes near the two sources, is not excluded by our observations. Comparing figures 22 and 23 we see that there is a substantial difference in the mean salt and sugar concentrations in the upper and lower layers between the two ends of the tank, though the net horizontal density gradients are very small. When these observations are compared with Run O, we conclude that the larger aspect ratio in Run S has produced vertical structures which are more strongly influenced by the source fluids at both ends of the tank.

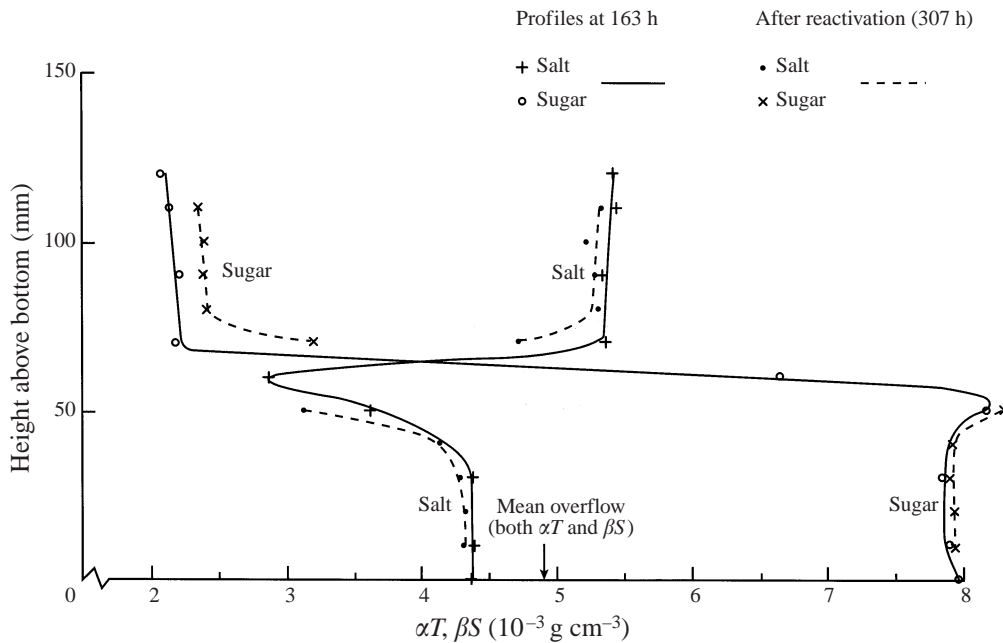


FIGURE 23. The vertical profiles measured in Run S corresponding to those in figure 22, but with sampling at the other end of the tank, 250 mm from the right-hand wall, nearer the sugar source.

### 9. Interpretation of the asymptotic salt and sugar distributions

As mentioned in the discussion of Run M, the asymptotic overall compositional distributions, i.e. the differences in salt and sugar concentrations between the top and bottom nearly uniform layers, correspond quite closely to a rundown 'diffusive' state. That is, the measurements are close to what would be achieved if a layer of salt solution with the initial density had been placed on top of a layer of sugar solution of equal density and depth, and double-diffusive transports through the interface had been allowed to proceed until all the potential energy in the salt field had been used. To demonstrate this, we have shown diagrammatically in figure 24 the changes in composition and density produced by the complete rundown across a diffusive interface with a flux ratio, sugar compared to the driving salt, of 0.5. (This value is close to that measured in one-dimensional salt/sugar experiments, but it has been chosen for illustration only; the values deduced from the present experiments will be presented later.) Also shown for comparison is the corresponding result for a finger interface, assuming a salt/sugar flux ratio of 0.9, again close to the measured value in one-dimensional experiments. These experimental values, and the papers in which they have been reported, are discussed in the review by Turner (1985).

Note that the measured flux ratios in the heat/salt system are approximately  $\beta F_S / \alpha F_T = 0.15$  for a diffusive interface with density ratios  $\beta \Delta S / \alpha \Delta T$  greater than 2 (Turner 1965) and  $\alpha F_T / \beta F_S = 0.65$  for a finger interface at values of  $\alpha \Delta T / \beta \Delta S$  close to 1, which are relevant in the ocean (McDougall & Taylor 1984). Thus the relative magnitudes of the flux ratios across the two types of interface are in the same sense as for the salt/sugar system, so that the deductions made in the following paragraph will be qualitatively true also for the oceanographically important heat/salt case.

It is seen that the final density difference, and also the salt and sugar distributions in the three runs discussed in §5, are indeed close to the rundown values for the

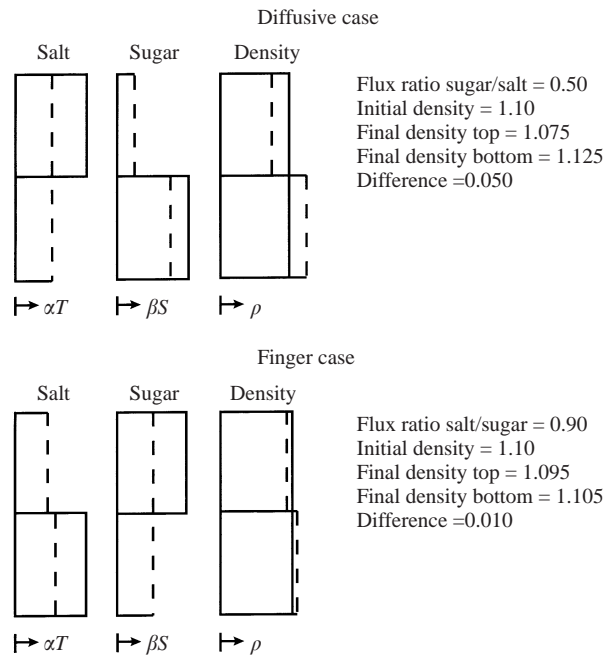


FIGURE 24. The densities in a two-layer system, before the experiments begin (solid vertical lines) and after complete rundown (dashed vertical lines), corresponding to the diffusive case with a flux ratio of 0.50 and the finger case with a flux ratio of 0.90.

diffusive case shown in figure 24. The density difference produced by rundown across a finger interface is much smaller. The system has in some way selected the state in which the release of potential energy is larger. Fingers are evidently not an efficient way of doing this, since the change in potential energy due to the transport of sugar downwards is nearly balanced by the transport of salt upwards in the counterflowing fingers, i.e. the flux ratio  $R_\rho$  is close to 1. (This result says nothing about the *rates* of density flux in the two cases. There are indications that this is faster for fingers at  $R_\rho$  near 1, as shown by the upward tilt of intrusions of sugar into a salt gradient (Turner 1978), and certainly fingers are very efficient at mixing both sugar and salt vertically.) At a diffusive interface, on the other hand, the faster diffusion of salt relative to sugar results in a larger net density change, with less compensation. This is far from being the whole story, since the evolution of our experiments is clearly not one-dimensional, and the three runs have quite different histories, especially in the early stages, as they develop towards the same asymptotic state. But before discussing the possible mechanisms in more detail, it will be instructive to interpret the results in terms of a one-dimensional 'diffusive interface' model.

Let the initial density due to salt or sugar (above the density of water) be  $\Delta\rho$ , and the contributions to the density difference between the two layers (of equal depth) in our experiments at any later time  $t$  be  $\alpha\Delta T$  and  $\beta\Delta S$ , respectively. If an amount  $n$  of salt (in density terms) has been transferred from the upper to the lower layer by time  $t$ , then the density difference due to salt becomes

$$\alpha\Delta T = \Delta\rho - 2n. \quad (1)$$

If  $x$  is the flux ratio, averaged over the whole time  $0-t$ , the corresponding density difference due to sugar, assuming that the transport is 'diffusive' and is driven by the

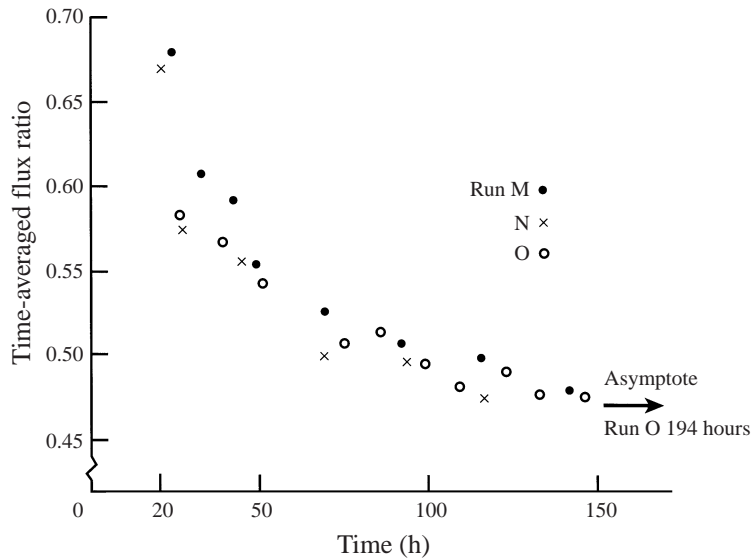


FIGURE 25. The evolution of the time-averaged flux ratio, calculated as described in the text assuming a one-dimensional rundown process, for the three Runs M, N and O.

salt transport, will be

$$\beta\Delta S = \Delta\rho - 2nx. \quad (2)$$

From the data used to plot figures 5 and 9, and the corresponding data for Run N,  $\Delta\rho$ ,  $\alpha\Delta T$  and  $\beta\Delta S$  in (1) and (2) are known, and hence  $n$  and  $x$ , consistent with the above simplistic assumptions, can be found as functions of time.

In figure 25 the flux ratio  $x$  is plotted for the three Runs M, N and O. The values before 20 h are scattered, and they are all above 0.9. Between 20 h and 150 h  $x$  falls steadily, and all runs are consistent with an approach to an asymptotic value of the time-averaged flux ratio of 0.470–0.480, consistent with the value deduced from Run O after 194 h. Since the transport processes are certainly not one-dimensional, through a fixed horizontal interface, the problem is now to explain why the overall structure evolves in this way.

The key to the explanation lies in the nature of the plumes which form near the sources of sugar and salt when they feed into an environment of different composition. These are visible in the photographs (for example in figure 13), but for greater clarity a close-up of a sugar source flowing into a homogeneous salt solution of the same density is reproduced here as figure 26. There is an immediate separation, with an upflow and a downflow forming, each driven by the more rapid diffusion of salt relative to sugar. Initially the excess diffusion of salt into a laminar sugar plume causes the plume to become heavier and sink, while the surroundings of the plume, having lost more salt (in density terms) than they have gained sugar, are lighter and rise. As the up- and downflows become stronger, and turbulent (without any increase in the source flow rate), this effect is increased by the formation of sheet-like boundaries between regions with different compositions. Further differential, coupled diffusion takes place across these sheets, thus contributing to the upward and downward transports of increasing volumes of fluid with different  $T$  and  $S$  properties. As was noted in the discussion of Run N in §5, it seems likely that a sugar plume

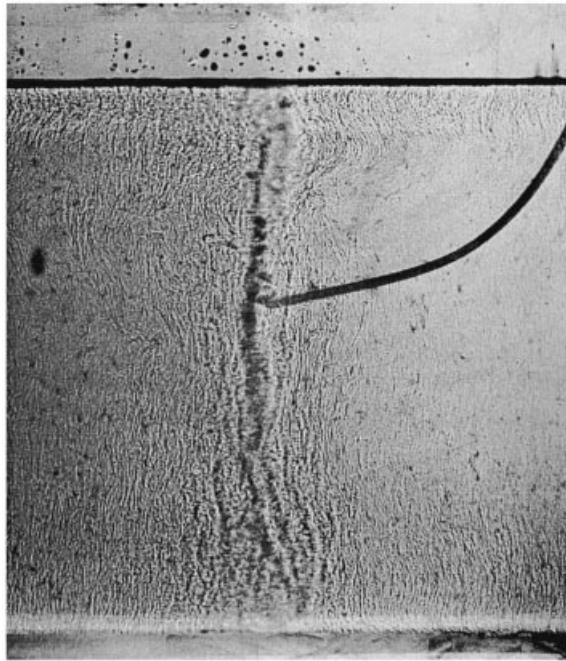


FIGURE 26. Close-up view (shadowgraph) of a plume of sugar solution flowing slowly into homogeneous salt solution of the same density. Double diffusion has caused separation and strong upward and downward convection, and the effect is enhanced when the flow becomes turbulent.

released into a homogeneous salt solution of the same density will behave differently from a salt plume in a sugar solution.

In the course of the evolution of the density structure, we have seen that both finger-favourable and diffusive stratifications are set up in various parts of the tank. But although the fluxes due to fingers may be locally vigorous, it is clear that the largest density differences result from the 'diffusive' transports. Even turbulent convection in isolated plumes sets up interfaces across which the maximum density increase is produced, although these interfaces are neither horizontal nor steady. The transport by fingers, on the other hand, does depend on the continuing existence of an ordered array of nearly vertical counterflowing cells which are easily disrupted, so that over time they cannot match the vertical density transport produced by the 'diffusive' processes.

Furthermore, the fluid breaking away from the edges of sharp interfaces, to produce convection in the relatively well-mixed layers on either side, takes the form of sheets, at both finger and diffusive interfaces. Figure 27 shows an interface just below a sugar source, in an experiment set up to illustrate this phenomenon, but with the sources and sink closer to the surface (so that we were modelling the lower half of the tank in the runs discussed above). These sheets also will be subject to differential 'diffusive' transports, and if the flux of buoyancy due to sugar is very strong the diffusion of salt into them may be enhanced while the sheath is carried along with the plume rather than convecting upwards. Salt advected from the other end of the tank also diffuses into the bottom of the thin finger interface, and increases the density of the boundary layer before it breaks away. Both of these processes will counteract the density and compositional transports produced by the finger interfaces themselves,



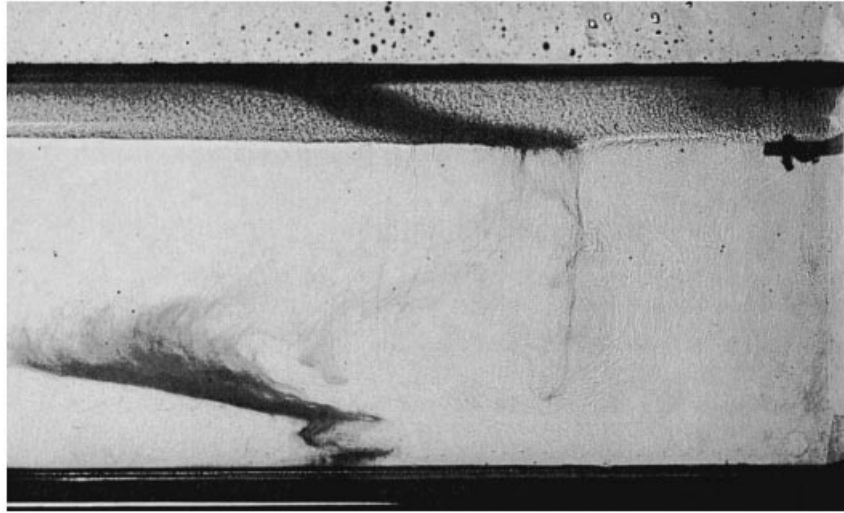


FIGURE 27. A dense sugar-rich plume breaking away from the bottom of a sharp finger interface, and transporting sugar downwards (as in Run M).

and can account for the large increase in the sugar concentration of the lower layer which was observed in Run M. Note in figure 27 the distortion of an originally vertical dye streak, inserted two minutes before the photograph was taken. This indicates that there has been a strong flow to the right at the level of the interface, feeding the separating sheet, and a large downward transport of sugar-rich fluid producing a deep lateral flow to the left.

Thus although we cannot monitor the individual processes continuously in all regions of the tank, a general principle seems to be established. It is reasonable to conclude that the overall mean state achieved over a long time is that in which the maximum potential energy has been released. This is the one-dimensional 'diffusive rundown' state, corresponding to a layer of salt solution above a layer of sugar solution of the same depth, each with the initial properties of the input fluids. Different inflow rates would require the argument to be modified to allow unequal layer depths. The 'final' or asymptotic state in the four quantitative experiments discussed here is clearly one of dynamic equilibrium, since the salinity at the top remains higher than that at the bottom. It is this unreleased potential energy in the salinity distribution which drives the continuing intrusive motions, and sustains the persistent fingering and diffusive layer structures in various regions of the tank.

## 10. Summary and discussion

In our exploration of the stratification and motions produced by two horizontally separated double-diffusive sources, many different phenomena have been documented. Though the use of salt and sugar sources rather than heat and salt, and the exclusion of other mixing processes, mean that the results cannot be directly applied to the ocean, this analogue system has on the other hand produced large and easily observed effects. We believe that the results can already be used to establish some general, more widely applicable principles.

The most striking difference between the effects of sources having different concentrations of a single stratifying component and double-diffusive systems lies in the

vertical stratification which can be achieved in the two cases. In both, the 'filling box' mechanism is operating to set up the vertical density gradient. With sources and ambient fluid containing just one diffusing solute, the final range of densities cannot lie outside the range of the input densities. But when there are double-diffusive transports, the range of densities can be very much larger than the initial density difference between the inputs, due to the net release of potential energy. Extreme examples of this are discussed in §§ 5 and 8, where it has been shown that large vertical density (and composition) gradients can be set up even when the sugar and salt source fluids and the fluid in the tank initially have exactly the same density.

The detailed behaviour is sensitive to the boundary conditions. The total vertical density difference achieved depends on the geometrical arrangement of sources and sinks. With the sink at mid-depth, a sharp interface develops there as fluid is removed, and two layers with weak gradients build up above and below this. The top layer becomes lighter and the bottom denser at about the same rates. If the sink is at the surface, approximately half this density difference is measured, since one half of the potential stratification has been removed. In all cases the mean properties of the 'overflow' fluid must be the (volume-averaged) mean of the two inputs, though in some geometries there can be a storage of input fluid during the evolution from the original ambient fluid. The properties of the two sources are not in themselves sufficient to determine the final state of stratification: experiments having the same arrangement of sources and sinks, and the same concentrations and flow rates of the input fluids, can reach different asymptotic states with different initial conditions in the tank.

The most detailed and instructive series of experiments were those with the sources and sink at mid-depth, and equal densities of the salt and sugar sources and the fluid in the tank. Starting with different tank fluids (pure salt, pure sugar or a mixture of the two) the three Runs M, N and O evolved to the same two-layer asymptotic state. The property distributions were 'diffusive', in the sense that the upper layer has an excess of salt (the more rapidly diffusing component) compared to the lower, while the sugar concentration was much higher in the lower layer. In each of the experiments it was clear, however, that the evolution was far from being steady or monotonic. Complicated two-dimensional intrusive motions persisted, even when the density structure seemed to be fully evolved. The remaining vertical salinity difference, combined with the horizontal gradients of salt and sugar, continued to drive convection and horizontal intrusions in the weakly stratified upper and lower layers, even when the mean vertical density difference was no longer increasing.

It is at first sight puzzling that the asymptotic mean concentrations in the two layers are close to the run-down state of a one-dimensional 'diffusive' experiment. In that case a homogeneous layer of salt solution is placed on top of a layer of sugar solution of the same density and the double-diffusive transports through the interface are allowed to run for a long time, with the density difference increasing because the potential energy released by the salt field is only partly used in lifting the sugar. This cannot be the mechanism in the two-source experiments we have described, in which horizontal shearing motions and intrusions are so prominent. But it has been argued that at every sharp interface, whether these are horizontal or vertical, steady or transient, across which there are differences of concentration of the two properties, salt will be transferred more rapidly than sugar, and the cumulative effect will be to maximize the release of potential energy.

The overall asymptotic property distributions cannot be primarily the result of salt fingering. Salt fingers release less net potential energy than a diffusive interface (since

the transport of salt upwards more nearly compensates for the energy release by the sugar field) and in any case a finger interface requires an ordered array of nearly vertical fingers to be effective. This same property means, however, that fingers are very effective at transporting sugar and salt vertically and making the distributions more nearly uniform. This argument about the relative importance of the transport across diffusive interfaces compared to salt fingers will also apply qualitatively to the heat/salt system. In that case too the transports of the two properties are more nearly compensating when there are fingers.

The detailed distributions of sugar and salt within the upper and lower layers do, however, depend on both finger and diffusive transport processes, and the two kinds of interfaces and layers are seen in the intrusions. The horizontal property anomalies set up by the salt and sugar sources at the two ends of the tank provide the driving energy for the large-scale shearing motions, and each source has a large effect on the environment into which the other is feeding. In the shorter tank, aspect ratio 5 : 1, the vertical distribution of properties near the salt source corresponds to what one would expect with a maximum of salt concentration at mid-depth (fingers in the upper layer and diffusive interfaces in the lower). Near the sugar source, however, salt fingers are prominent in both layers, indicating that sugar has been transported to the surface by convection, above a layer of salt advected along the lower part of the upper layer from the other end of the tank. Thus the vertical convection near the salt and sugar sources must be different, not just antisymmetric. In the longer tank, aspect ratio 15 : 1, the effect of the local source dominates over the advection from the remote source, at both ends of the tank. The concentration distributions and structures at the end near the sugar source do correspond to a maximum of sugar concentration near the interface.

Finally, we again draw attention to the ocean observations referred to in the Introduction. It seems clear that the phenomena described by Schmitt (1994) and by Carmack *et al.* (1997) cannot be explained in terms of density differences alone, and that they contain many features which are related to observations in our laboratory experiments. Though no direct application of our results is possible or appropriate at this time, we believe that two-dimensional double-diffusive effects certainly need to be included in order to interpret their data. It is not surprising that if a significant physical process is left out, one will get the wrong, or at least an incomplete, picture of an oceanographic phenomenon.

We wish to thank Derek Corrigan and Tony Beasley for their assistance in setting up and carrying out the experiments, and Ross Wylde-Browne for the preparation of the photographs and diagrams. We are very grateful to Eddy Carmack for his interest and inputs, and for allowing us to reproduce figure 1.

#### REFERENCES

- BAINES, W. D. & TURNER, J. S. 1969 Turbulent buoyant convection from a source in a confined region. *J. Fluid Mech.* **37**, 51–80.
- CARMACK, E., AAGAARD, K., SWIFT, J., PERKIN, R., MCLAUGHLIN, F., MACDONALD, R., JONES, P., SMITH, J., ELLIS, K. & KILIUS, L. 1997 Changes in temperature and tracer distributions within the Arctic Ocean: Results from the 1994 Arctic Ocean Section. *Deep-Sea Res.* **44**, 1487–1502.
- CHEN, C. F. & CHEN, F. 1997 Salt-finger convection generated by lateral heating of a solute gradient. *J. Fluid Mech.* **352**, 161–176.
- HUPPERT, H. E. & TURNER, J. S. 1980 Ice blocks melting into a salinity gradient. *J. Fluid Mech.* **100**, 367–384.

- MAXWORTHY, T. 1997 Convection into domains with open boundaries. *Ann. Rev. Fluid Mech.* **29**, 327–371.
- MCDUGALL, T. J. & TAYLOR, J. R. 1984 Flux measurements across a finger interface at low values of the stability ratio. *J. Mar. Res.* **42**, 1–14.
- PHILLIPS, O. M. 1966 On turbulent convection currents and the circulation in the Red Sea. *Deep-Sea Res.* **13**, 1149–1160.
- PIERCE, D. W. & RHINES, P. B. 1996 Convective building of a pycnocline: laboratory experiments. *J. Phys. Oceanogr.* **26**, 176–190.
- ROSSBY, H. T. 1965 On thermal convection driven by non-uniform heating from below: an experimental study. *Deep-Sea Res.* **12**, 9–16.
- RUDDICK, B. R., PHILLIPS, O. M. & TURNER, J. S. 2000 A laboratory and quantitative model of finite-amplitude thermohaline intrusions. *Dyn. Atmos. Oceans*. Special Issue, papers presented at 1998 AGU Ocean Sciences Meeting, San Diego. (In press.)
- RUDDICK, B. R. & SHIRTCLIFFE, T. G. L. 1979 Data for double diffusers: Physical properties of aqueous salt-sugar solutions. *Deep-Sea Res.* **26**, 775–787.
- RUDDICK, B. R. & TURNER, J. S. 1979 The vertical lengthscale of double-diffusive intrusions. *Deep-Sea Res.* **26**, 903–913.
- SCHMITT, R. W. 1994 Double diffusion in oceanography. *Ann. Rev. Fluid Mech.* **26**, 255–285.
- TURNER, J. S. 1965 The coupled turbulent transports of salt and heat across a sharp density interface. *Intl J. Heat Mass Transport* **38**, 375–400.
- TURNER, J. S. 1978 Double-diffusive intrusions into a density gradient. *J. Geophys. Res.* **83**, 2887–2901.
- TURNER, J. S. 1985 Multicomponent convection. *Ann. Rev. Fluid Mech.* **17**, 11–44.
- TURNER, J. S. 1998 Stratification and circulation produced by heating and evaporation on a shelf. *J. Mar. Res.* **56**, 885–904.
- TURNER, J. S. & CHEN, C. F. 1974 Two-dimensional effects in double-diffusive convection. *J. Fluid Mech.* **63**, 577–592.
- WONG, A. B. D. & GRIFFITHS, R. W. 2000 Stratification and convection produced by multiple turbulent plumes. *Dyn. Atmos. Oceans*. Special Issue, papers presented at 1998 AGU Ocean Sciences Meeting, San Diego. (In press.)